Scattering of two-dimensional dark solitons by a single quantum vortex in a Bose-Einstein condensate

Lev A. Smirnov* and Alexander I. Smirnov
Institute of Applied Physics of the Russian Academy of Sciences, Nizhny Novgorod 603950, Russia
and Lobachevsky State University of Nizhny Novgorod, Nizhny Novgorod 603950, Russia
(Received 8 May 2015; published 31 July 2015)

We study the process of scattering of two-dimensional dark solitons, and their vortex-antivortex pairs as a specific case, by a single quantum vortex in a Bose-Einstein condensate with repulsive interaction between atoms. An asymptotic theory describing the dynamics of such solitonlike structures in a smoothly inhomogeneous flow of ultracold Bose gas is developed. An analytical expression for the angle of scattering of two-dimensional dark solitons (including vortex pairs) by a single-phase singularity is obtained in the limit of large impact parameters. All theoretical concepts are confirmed by numerical calculations performed directly within the Gross-Pitaevskii equation. It is shown that for small impact parameters, the considered solitonlike structures interact inelastically with the core of a single quantum vortex, scattering over large angles and radiating sound waves.

DOI: 10.1103/PhysRevA.92.013636 PACS number(s): 03.75.Lm, 03.75.Kk, 03.75.Hh, 67.85.De

I. INTRODUCTION

The dynamics of vortex structures and their interaction with each other in many ways determine the key aspects of the evolution of a cloud of ultracold Bose gas with repulsive interaction between atoms. *Quantum vortices* (*topological defects* or *phase singularities*) are associated with the breaking of the superfluidity mode and the transition of the Bose-Einstein condensate (BEC) to the turbulent state [1–15]. To understand and describe such a transition, it is most important to make a maximum progress in solving the model problems of motion for interacting vortex structures. This issue has been addressed in a fairly large number of papers (see, e.g., [16–25]), which use, as a rule, the incompressible fluid model of point vortices. However, using this model is not always justified for the BEC, especially when the processes leading to turbulence are studied.

The reasons for the generation of vortices in an ultracold Bose gas are very diverse. They are formed in the BEC flows behind the obstacles, whose role is usually played by laser beams [9–15,26], because of the development of a modulation instability of elongated (quasi-one-dimensional) inhomogeneities [9,27,28], at the dispersive shock-wave front [29–32], etc. Quantum vortices tend to occur in *vortex-antivortex pairs*. Such pairs in a homogeneous BEC are a specific case of two-dimensional (2D) dark solitons [33–42] moving along straight lines with constant velocities. In the absence of an external potential, these solitons are localized solutions of the Gross-Pitaevskii (GP) equation, which, in dimensionless variables, coincides with the nonlinear Schrödinger (NLS) equation with a defocusing nonlinearity [43–45].

Numerical calculations [40,41] show that in a smoothly inhomogeneous condensate, where the distance between the vortex and antivortex is much smaller than the characteristic scale of the inhomogeneity of the medium, the vortex pairs are close in structure to the corresponding 2D dark solitons. However, in this case, the shape of the solitonlike structures is reconstructed slowly (in particular, the distance between topological defects that are opposite in sign changes), and they move with acceleration, generally along curved, rather than straight, paths.

In our previous works [40,41], we analyzed in detail the behavior of 2D dark solitons in a smoothly inhomogeneous flow-free BEC, whose stationary density distribution is formed and maintained by the potential of the external forces acting on the condensate (e.g., the confining trap potential). In this paper, we consider specific features of the dynamics of such solitonlike structures (including vortex pairs) in an inhomogeneous flow of ultracold Bose gas, paying particular attention to their scattering by a single quantum vortex. For the vortex pairs incident on an isolated topological defect in the BEC, this problem has partly been analyzed numerically [46–48]. It should also be mentioned that for long characteristic distances between the phase singularities, their interaction can in some cases be described using the approximation of an incompressible fluid and the model of point vortices, whose dynamics has been studied extensively in hydrodynamics since the beginning of the last century. As was shown by Poincaré [49,50], the nonlinear Hamiltonian system of equations for the motion of three point vortices is always integrable for an arbitrary set of vortex strengths. The numerous solutions of this system were studied in detail by Gröbly [51,52]. In particular, he considered the problem of scattering of a vortex pair by a vortex. However, as applied to BEC, the theory developed by Gröbly, which neglects the condensate compressibility, has only a limited scope of application.

In some papers, their authors studied the processes of scattering of *sound waves* by a quantum vortex (see, e.g., [53–57]) and interaction of one-dimensional (1D) dark solitons with a topological defect [58–60]. Our studies are in the natural continuation of those publications.

This paper is organized as follows. It is divided into two main parts (Secs. II and III). In Sec. II, we develop the variational approach to the problem of the behavior of a 2D dark soliton in a smoothly inhomogeneous cloud of condensate with stationary flows. First of all (in Sec. II A), we formulate the basic equation of the BEC dynamics with repulsive

*smirnov_lev@appl.sci-nnov.ru

interaction between atoms. Then (in Secs. II B and II C), we report on the stationary quantum vortices and 2D dark solitons moving at constant velocities. In particular, we give an analytical approximation, which was obtained in [40,41], for the dependence of the momentum of such a soliton on its energy. In Sec. II D, basing on the variational approach, we develop an asymptotic description of the dynamics of a solitary localized density drop, which is similar to a 2D dark soliton, in a smoothly inhomogeneous flow of BEC and deduce a system of ordinary differential equations governing the motion of a quasiparticle that can be assigned to the considered solitonlike structure. In Sec. III, using the developed asymptotic theory and direct numerical simulation within the framework of the GP equation, we analyze the problem of scattering of a 2D dark soliton (including a vortex pair) by a single quantum vortex. We deliberately neglect the impact of the trap potential, which confines the cloud of ultracold Bose gas, on the condensate and focus on features related first of all with the interaction of nonlinear wave structures. Such a neglect of external potential forces is justified for very smooth traps. In addition, this assumption is certainly fulfilled in cases where the technologies and methods proposed and demonstrated in the experiments [61–63], in which a quasiuniform distribution of the BEC density was created in a fairly large region of space, are used. In Sec. III C, we pay special attention to sound waves generation during collision of 2D dark solitons with the initially isolated topological defect. In Sec. III D, we use numerical simulation to study the dependencies of the scattering angle, at which the solitonlike structure is incident on a single quantum vortex, on the impact distance. The limit of large impact distances is also considered analytically and an expression that relates the scattering angle and the parameters of a 2D dark soliton at the start point is obtained. In Conclusions (Sec. IV), we summarize the main results of our work.

II. VARIATIONAL APPROACH TO THE PROBLEM OF THE DYNAMICS OF 2D DARK SOLITONS IN A SMOOTHLY INHOMOGENEOUS BEC WITH FLOW

A. Mean-field approximation for the Bose gas at an absolute zero temperature: Basic equation of the BEC dynamics

The BEC dynamics will be described in the *mean-field approximation*, according to which the system of a macroscopic number of identical bosons in condensed state is characterized by a unified *classical wave function* $\Psi(\mathbf{r},t)$, which satisfies the GP equation [43–45]. This equation for an ultracold Bose gas with repulsive interaction between atoms in dimensionless variables has the following form [40,43–45]:

$$i\frac{\partial\Psi}{\partial t}+\frac{1}{2}\Delta\Psi+(1-|\Psi|^2)\Psi=V_{ext}(\mathbf{r})\Psi. \tag{1}$$

Here, the time t, the coordinates $\mathbf{r}$, the function $\Psi(\mathbf{r},t)$, and the potential $V_{ext}(\mathbf{r})$ of the external forces acting on the condensate were normalized in such a way that the dimensionless chemical potential of the ground state is equal to unity [40,43–45]. From Eq. (1), one can also pass, using *Madelung transform* $\Psi(\mathbf{r},t)=\psi(\mathbf{r},t)\exp[i\theta(\mathbf{r},t)]$, to hydrodynamic equations of compressible inviscid fluid:

$$\frac{\partial\psi^2}{\partial t}+\mathrm{div}(\psi^2\nabla\theta)=0, \tag{2}$$

$$\frac{\partial\theta}{\partial t}+\frac{1}{2}(\nabla\theta)^2=1-\psi^2+\frac{\Delta\psi}{2\psi}-V_{ext}(\mathbf{r}), \tag{3}$$

where $\psi(\mathbf{r},t)$ and $\theta(\mathbf{r},t)$ are the real-valued functions of the coordinates and time, which have a distinct physical meaning, namely, $n(\mathbf{r},t)=\psi^2(\mathbf{r},t)$ is the density of BEC atoms and $\mathbf{v}(\mathbf{r},t)=\nabla\theta(\mathbf{r},t)$ is their velocity. The term $\Delta\psi/2\psi$ is associated with a specific quantity, the so-called *quantum-mechanical pressure*.

In this paper, we focus on a 2D problem to which the analysis of the behavior of the Bose condensates in *disklike traps* reduces [40,43–45]. The potential of such traps is fairly sharply localized with respect to the coordinate z and gradually varies with respect to two other coordinates, x and y. Thus, the structure of the BEC cloud along the z axis can be assumed fixed, and after the factorization procedure [40,43–45] in Eqs. (1)–(3), it suffices to consider only the dependence of the functions on the 2D vector $\mathbf{r}=(x,y)$.

In the homogeneous BEC, where $V_{ext}(\mathbf{r})=0$, there are nonlinear wave structures, both at rest and moving at constant velocities, in the form of single quantum vortices [43–45] and 2D dark solitons [33–42], respectively. These structures are described by solitary solutions of the GP equation (1) and in many respects determine the long-term evolution of the cloud of ultracold Bose gas.

B. Stationary quantum vortices

The presence of *quantum vortices* (*topological defects*, or *phase singularities*) is one of the most characteristic features of superfluid systems [1,9,43–45], which include, in particular, BEC of rarefied ultracold gases with repulsive interaction between atoms. Velocity field circulation along a closed path enveloping the vortex center is equal to $2\pi\varkappa$, where $\varkappa$ is an integer, which is often called an *azimuthal index* or a *topological charge*. Accordingly, when going around these lines, the phase of the macroscopic wave function of a superfluid system changes to $2\pi\varkappa$.

The vortices with azimuthal indices $|\varkappa|>1$ fall into $|\varkappa|$ vortices that are stable in the class of 2D solutions, with topological charges that are unit in modulus [64–66]. Therefore, hereafter we assume that $\varkappa=\pm1$. For $\varkappa=+1$ and -1, the condensate is counterclockwise (vortex) or clockwise (antivortex) rotated.

In the initially homogeneous BEC, where $V_{ext}(\mathbf{r})=0$, in the polar coordinate system r, φ connected with the central point, stationary wave functions $\Psi_v^{\pm}(\mathbf{r})$ of the vortex and antivortex, respectively, have a fairly simple form, namely, $\Psi_v^{\pm}(\mathbf{r})=\psi_v(r)\exp(\pm i\varphi)$, where the phase $\pm\varphi$ determines the presence of a singular (for $r=0$) vortex flow $\mathbf{v}_v^{\pm}(\mathbf{r})=\pm\boldsymbol{\varphi}_0/r$ ($\boldsymbol{\varphi}_0$ is the unit vector of the angular variable φ) and the amplitude $\psi_v(r)$ in both cases satisfies the ordinary differential equation [1,43–45]

$$\frac{1}{2}\left(\frac{d^2\psi_v}{dr^2}+\frac{1}{r}\frac{d\psi_v}{dr}-\frac{1}{r^2}\psi_v\right)+\left(1-\psi_v^2\right)\psi_v=0 \tag{4}$$

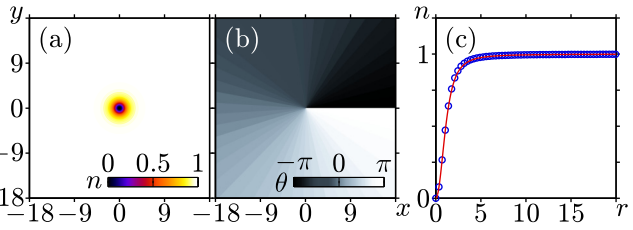

FIG. 1. (Color online) Distributions (a) of the density and (b) of the phase of the BEC wave function in the presence of a single quantum vortex with $\varkappa=+1$ located at the center of the Cartesian coordinate system x, y. (c) Gives a comparison of the Padé approximation (7) (red solid line) for the dependence $n_v(r)$ with the results of numerical calculation (unshaded blue markers) using Eq. (4) and the boundary conditions $\psi_v(0)=0$ and $\psi_v(\infty)=1$.

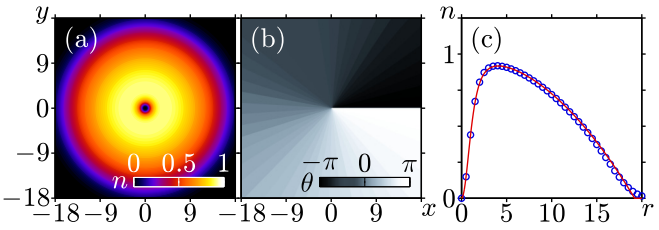

FIG. 2. (Color online) Distributions (a) of the density and (b) of the phase of the wave function of the BEC confined in the axially symmetric harmonic potential (8) with $\omega_r\approx 0.0736$ in the presence of a single quantum vortex with $\varkappa=+1$ at the trap center. (c) Gives a comparison of the approximation (9) (red solid line) for the dependence $n_v(r)$ with the results of numerical calculation (unshaded blue markers) directly within the GP equation (1).

with the boundary conditions $\psi_v(0)=0$ and $\psi_v(\infty)=1$, which ensure that $\psi_v(r)$ is continuous at the point $r=0$ and the condensate density reaches unity at $r\to\infty$.

We note that the vicinity of the point $r=0$, where the density $n_v(r)=\psi_v^2(r)$ of Bose particles in the vortex solution differs markedly from the density of a homogeneous background condensate, i.e., $n_v(r)\ll 1$, and the quantum-mechanical pressure is significant, is called the *core* of a quantum vortex. At the boundary of this region, the speed of the flow created by a topological defect in the BEC becomes of the order of the sound speed. A characteristic size of the core is close to the correlation radius (equal to unity in the dimensionless variables being used), which in the case of a rarefied ultracold Bose gas is great compared with the interatomic spacing. Therefore, the structure of the vortex and antivortex can be described macroscopically.

The function $\psi_v(r)$, which satisfies Eq. (4) and the corresponding boundary conditions, can be found only numerically (Fig. 1). However, it is easy to establish the asymptotic behavior of the dependence $\psi_v(r)$ for $r\to 0$ and $r\to\infty$ [37,67]. In the first case, where $r\ll 1$, we have

$$\psi_v(r\ll 1)=\alpha_1 r-\frac{\alpha_1}{4}r^3+\frac{\alpha_1\left(4\alpha_1^2+1\right)}{48}r^5+o(r^7) \quad (5)$$

with $\alpha_1=0.824\,177\,059$. Outside the core of the quantum vortex (antivortex), and at sufficiently long distances $r\gg 1$ from the core, the amplitude $\psi_v(r)$ of the BEC wave function is determined by the following expression:

$$\psi_v(r\gg 1)=1-\tfrac{1}{4}r^{-2}-\tfrac{9}{32}r^{-4}-\tfrac{161}{128}r^{-6}+o(r^{-8}). \quad (6)$$

Using asymptotic forms (5) and (6), the stationary distribution of the density $n_v(r)$ of a condensate with vortex (antivortex) can be fit with the *Padé approximation* [67]

$$n_v^{[2/2]}(r)=\frac{a_1r^2+a_2r^4}{1+b_1r^2+b_2r^4},\quad a_1=\alpha_1^2,$$
$$b_1=\frac{3\alpha_1^2}{\sqrt{2}\left(2-\alpha_1^2\right)},\quad a_2=b_2=\frac{\alpha_1^2\left(2\alpha_1^2-1\right)}{4\left(2-\alpha_1^2\right)}, \quad (7)$$

which reproduces coefficients up to terms of order r^3 in expansion (5) and up to terms of order r^{-2} in expansion (6), i.e., gives the correct behavior of $n_v(r)$ simultaneously with $r\to 0$ and $r\to\infty$. Furthermore, a comparison shows [see Fig. 1(c) and [67]] that the dependence $n_v^{[2/2]}(r)$ calculated by formula (7) is everywhere close to the density $n_v(r)$ of an ultracold Bose gas with phase singularity, which was calculated using the numerical solution of Eq. (4).

When a quantum vortex or antivortex is located at the center of the BEC cloud confined in the x, y plane by an *axially symmetric harmonic potential*

$$V_{ext}(r)=\omega_r^2r^2/2, \quad (8)$$

the phases of the corresponding stationary wave functions $\Psi_v^{\pm}(\mathbf{r})$ in the polar coordinate system r, φ will still be equal to $\pm\varphi$, and their amplitudes $\psi_v(r)$ in both cases will satisfy Eq. (4) with a nonzero right-hand side, which is equal to $V_{ext}(r)\psi_v(r)$, and the boundary conditions $\psi_v(0)=0$ and $\psi_v(\infty)=0$. This boundary-value problem, as the one considered above, can be solved only numerically [see Fig. 2 and [68–70]]. However, for a smooth potential $V_{ext}(r)$ of the form (8) with $\omega_r\ll 1$ in this space domain, where $1-V_{ext}(r)>0$, the density $n_v(r)$ of the condensate can be adequately described by the following approximation [see Fig. 2(c) and [68–70]]:

$$n_v^{\mathrm{TF}}(r)=[1-V_{ext}(r)]\,n_v^{[2/2]}(r). \quad (9)$$

The first term in this factorized representation is the Thomas-Fermi (TF) approximation for the density distribution of a condensate with repulsive interaction between atoms, which is enclosed in a large-scale trap [43–45].

Note that a quantum vortex (antivortex) will be at rest only if the related phase singularity is located at the point coinciding with the center of the potential (8). Otherwise, when the topological defect is away from this point, the quantum vortex will rotate around it, with frequency determined by ω_r (see, e.g., [1,16,70–75]). However, this effect is beyond the scope of this paper and is not discussed here in detail.

C. 2D dark solitons in a homogeneous BEC

It is easy to show that the BEC energy concentrated within the region of radius R with a topological defect at the center increases logarithmically with increasing R [43,44,67]. However, in a homogeneous condensate, there are stable vortex structures having an ultimate energy. The simplest of these are the vortex-antivortex pairs, which are a particular case of 2D dark solitons of the GP equation (1) with $V_{ext}(\mathbf{r})=0$.

Two-dimensional (2D) dark solitons are the localized density drops moving at constant subsonic velocities $\bar{v}$ against the background of a unit-density BEC [33–42]. Their wave functions $\bar{\Psi}_s(\xi, y, \bar{v})$ satisfy the stationary NLS equation

$$-i\bar{v}\frac{\partial\bar{\Psi}_s}{\partial\xi}+\frac{1}{2}\frac{\partial^2\bar{\Psi}_s}{\partial\xi^2}+\frac{1}{2}\frac{\partial^2\bar{\Psi}_s}{\partial y^2}+(1-|\bar{\Psi}_s|^2)\bar{\Psi}_s=0 \quad (10)$$

with the boundary condition $\bar{\Psi}_s[(\xi^2+y^2)\to\infty]\to 1$.

These solitary structures can also be considered as a one-parameter family of solutions of the variational problem $\delta(\mathcal{H}-\bar{v}\mathcal{P}_x)=0$, where

$$\mathcal{H}=\frac{1}{2}\int_{-\infty}^{+\infty}dy\int_{-\infty}^{+\infty}d\xi\,[|\nabla\Psi|^2+(1-|\Psi|^2)^2], \quad (11)$$

$$\mathbf{P}=\frac{i}{2}\int_{-\infty}^{+\infty}dy\int_{-\infty}^{+\infty}d\xi\,(\Psi\nabla\Psi^*-\Psi^*\nabla\Psi) \quad (12)$$

are the Hamiltonian and the momentum of condensate, respectively. This variational formulation implies the following relations [35,40,41]:

$$\begin{aligned}\bar{\mathcal{E}}&=\int_{-\infty}^{+\infty}dy\int_{-\infty}^{+\infty}d\xi\left|\frac{\partial\bar{\Psi}_s}{\partial\xi}\right|^2,\\ \bar{\mathcal{E}}-\bar{v}\bar{\mathcal{P}}&=\int_{-\infty}^{+\infty}dy\int_{-\infty}^{+\infty}d\xi\left|\frac{\partial\bar{\Psi}_s}{\partial y}\right|^2,\\ \bar{v}\bar{\mathcal{P}}&=\int_{-\infty}^{+\infty}dy\int_{-\infty}^{+\infty}d\xi(1-|\bar{\Psi}_s|^2)^2,\\ \bar{v}&=\frac{d\bar{\mathcal{E}}}{d\bar{\mathcal{P}}}<\frac{\bar{\mathcal{E}}}{\bar{\mathcal{P}}}.\end{aligned} \quad (13)$$

Here, $\bar{\mathcal{E}}=\mathcal{H}_s$ and $\bar{\mathcal{P}}=\mathcal{P}_{sx}$ are the soliton energy and momentum, respectively. In this case, $\bar{v}$, $\bar{\mathcal{P}}$, and $\bar{\mathcal{E}}$ *are uniquely related to each other*.

In Refs. [33–35,37,40,41], the properties of 2D dark solitons were considered in detail within the framework of Eq. (10). In particular, the features of their inner structure as functions of the quantity $\bar{v}$, which plays the role of the problem parameter, were analyzed there. When $0<\bar{v}<0.61$, the solitons are *vortical*, and for $0.61\leqslant\bar{v}<1$ are *vortex free*. In the first case [see Figs. 3(a) and 3(d), 3(b) and 3(e)], they are the so-called *vortex-antivortex pairs*, in which the condensate density at two points located on the line perpendicular to the direction of motion becomes zero. The phase of the wave function $\bar{\Psi}_s(\xi, y, \bar{v})$ of BEC when going around these points changes to $\pm 2\pi$. As the speed $\bar{v}$ increases, the energy $\bar{\mathcal{E}}$ of a 2D dark soliton decreases, and the phase singularities in it converge. For the *critical energy* $\bar{\mathcal{E}}_*=7.59$, which corresponds to the *critical velocity* $\bar{v}_*=0.61$, the topological defects merge, so that instead of the vortex pair, there forms a vortex-free soliton, in which the condensate density nowhere vanishes and jumps by $\pm 2\pi$ are absent in the phase distribution [see Figs. 3(c) and 3(f). In the weakly nonlinear limit, where the speed $\bar{v}$ tends to the sound velocity, i.e., $1-\bar{v}\ll 1$, vortex-free solitons are close in structure to solitary solutions of the Kadomtsev-Petviashvili (KP) equation [76–78].

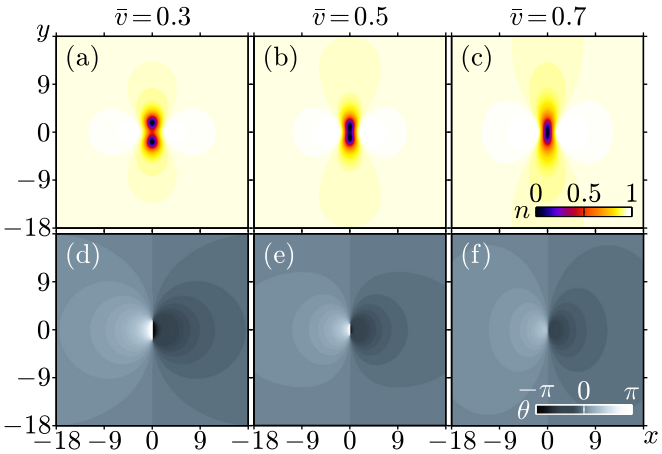

FIG. 3. (Color online) Distribution (a)–(c) of the condensate density and (d)–(f) of the phase of the BEC wave function in 2D dark solitons for three values of the soliton velocity $\bar{v}$, namely, (a), (d) $\bar{v}=0.3$, (b), (e) $\bar{v}=0.5$, and (c), (f) $\bar{v}=0.7$. For $\bar{v}=0.3$ and 0.5, these solitons have the form of vortex pairs, in which the condensate density at two points vanishes [see fragments (a) and (b)], and the phase of the BEC wave function $\Psi_s(\xi, y)$ when going around these points changes to $\pm 2\pi$ [see fragments (d) and (e)]. For the velocity $\bar{v}=0.7$, a 2D dark soliton is vortex free, i.e., the density of ultracold Bose gas in it nowhere vanishes [see fragment (c)], while the phase of the wave function $\Psi_s(\xi, y)$ changes gradually [see fragment (f)].

Note that for the dependence of the momentum $\bar{\mathcal{P}}$ of a 2D dark soliton on its energy $\bar{\mathcal{E}}$, which was calculated by numerically solving the stationary equation (10), we found a fairly simple *analytical approximation* [40,41]

$$\bar{\mathcal{P}}(\bar{\mathcal{E}})=\wp(\bar{\mathcal{E}})\sinh[\bar{\mathcal{E}}/\wp(\bar{\mathcal{E}})], \quad (14)$$

$$\wp(\bar{\mathcal{E}})=2\pi+(2\pi/3)\exp[-(\bar{\mathcal{E}}/9.8)^2], \quad (15)$$

which has a high accuracy. In other words, we have constructed a *nonlinear dispersion relation* for the considered soliton excitations in a homogeneous BEC.

D. Asymptotic description of the dynamics of 2D dark solitons in a smoothly inhomogeneous vortex flow of BEC

A fairly universal and frequently used approach to solving the problems of the dynamics and interaction of solitons (or, more precisely, quasisolitons) in different nonlinear models close to integrable is the *variational method* [78–80]. This approach permits one to analyze the processes of propagation and collision of solitary waves in terms of slow evolution of their parameters, the so-called *collective coordinates*. The main idea of this method is as follows. First, it is needed to select a particular approximation that describes most adequately and correctly the shape of nonlinear structures and substitute it into the *Lagrange function density*. Then, one should calculate the *averaged Lagrangian*, assuming that during integration the parameters of solitonlike structures change adiabatically gradually in time, and vary the resulting expression for the collective coordinates. This strategy is

similar to the approach proposed by Whitham and which he used for a study of the behavior of the trains of periodic traveling waves (often called cnoidal waves) [81].

It should be specially mentioned that some of the disturbances can break the Hamiltonian nature of the undisturbed nonlinear equations having solutions in the form of solitons. Dissipative effects and external nonconservative forces can be taken into account when the Lagrangian is varied by introducing generalized forces corresponding to the collective coordinates, as is done in classical mechanics (see, e.g., [82,83]).

Whitham's method has repeatedly demonstrated its high efficiency and expediency in the study of the dynamics and interaction of solitary waves in a variety of the nonlinear physical models described, in particular, by the sine-Gordon (SG) and Korteweg–de Vries (KdV) equations, as well NLS equations in the presence of different types of disturbances (including the dissipative ones) and smooth inhomogeneities [78–80]. We emphasize that the variational method was used for a study of the behavior of 1D dark solitons and ring dark solitons (see, e.g., [45,82,84–86]) in the BEC confined in a parabolic trap [45,87], as well as for the analysis of their modulation instability [88,89]. However, such a theory for 2D dark solitons has not existed to date. Therefore, in this section we will develop the ideology outlined above in relation to the problem of scattering of such solitary density drops (including vortex pairs) by a single quantum vortex. This procedure is not difficult to generalize to other cases where we are talking about the behavior of localized structures in an ultracold Bose gas with repulsive interaction between atoms.

So, let a 2D dark soliton moving in the general case against the background of a smoothly inhomogeneous BEC be incident on a single quantum vortex with the topological charge $\varkappa = +1$. Note that using symmetry considerations, all the results obtained in the following can easily be extended to the case of a phase singularity with the azimuthal index opposite in sign $\varkappa = -1$, i.e., an antivortex. In the space domain where the characteristic size Λ_s of a 2D dark soliton is small compared with the distance r_s to the vortex center, i.e., $\Lambda_s \ll r_s$, it is possible to introduce a *small parameter* $\mu = \Lambda_s/r_s \ll 1$, which characterizes smooth variations in the vortex velocity field on the scale Λ_s. The wave function $\Psi(\mathbf{r},t)$ of the condensate can conveniently be represented in the form of the product

$$\Psi(\mathbf{r},t) = \Psi_v(\mathbf{r})\Phi(\mathbf{r},t), \tag{16}$$

where $\Phi(\mathbf{r},t)$ is the complex function of the coordinates $\mathbf{r}$ and time t, $\Psi_v(\mathbf{r})$ is the stationary wave function of a single quantum vortex, which was discussed in Sec. II B (the upper index $^+$ is omitted to avoid a cumbersome writing in what follows). That the function $\Psi_v(\mathbf{r})$ corresponding to the isolated topological defect was extracted as one of the factors reflects the fact that a 2D dark soliton transiting at long distances r_s ($r_s \gg \Lambda_s$) from the center of the phase singularity disturbs very weakly the structure of the quantum vortex and the flow it created. Therefore, the inverse effect of such a disturbance on the dynamics of the solitonlike structure can be neglected. Upon substitution of expression (16) into the GP equation (1) for the second factor $\Phi(\mathbf{r},t)$ describing the behavior of a 2D dark soliton in a smoothly inhomogeneous vortex flow of BEC, we obtain the nonlinear dynamic equation

$$i\frac{\partial\Phi}{\partial t} + \frac{1}{2}\Delta\Phi + n_v(\mathbf{r})(1-|\Phi|^2)\Phi + \left\{i\mathbf{v}_v(\mathbf{r}) + \frac{1}{2}\nabla[\ln n_v(\mathbf{r})]\right\}\cdot\nabla\Phi = 0. \tag{17}$$

Here, $\mathbf{v}_v(\mathbf{r})$ is the velocity field created in an ultracold Bose gas by an isolated topological defect, and $n_v(\mathbf{r})$ determines the inhomogeneous distribution of the density of the background condensate with a single quantum vortex. Equation (17) is essentially an NLS equation with smoothly inhomogeneous coefficients. The *Lagrange function density* corresponding to this equation (and its complex-conjugate counterpart) has the following form:

$$\mathcal{L}(\Phi,\Phi^*) = \frac{i}{2}n_v(\mathbf{r})\left\{\Phi\left[\frac{\partial}{\partial t} + \mathbf{v}_v(\mathbf{r})\cdot\nabla\right]\Phi^* - \text{c.c.}\right\} + \frac{n_v(\mathbf{r})}{2}|\nabla\Phi|^2 + \frac{n_v^2(\mathbf{r})}{2}(1-|\Phi|^2)^2. \tag{18}$$

Now, the dynamics of 2D dark solitons in a smoothly inhomogeneous vortex flow can be described using the variational method based on averaging of expression (18) over the so-called fast variables.

We assume that the solitonlike structure in the form of a density drop moves against the inhomogeneous background stipulated by the presence of a single quantum vortex in the center of the BEC cloud confined in the trap along a smoothly curved path $\mathbf{r}_s(t)$ with slowly varied velocity $\mathbf{v}_s(t) = \dot{\mathbf{r}}_s(t)$. By virtue of the condition $\Lambda_s \ll r_s$, at any arbitrary moment of time t such a quasisoliton excitation is close in structure to the corresponding solitary solution $\Phi_s(\mathbf{r}-\mathbf{r}_s,\mathbf{v}_s)$ of Eq. (17), in which instead of the scalar function $n_v(\mathbf{r})$ of the space variables $\mathbf{r}$ and the vector field $\mathbf{v}_v(\mathbf{r})$ we substituted for each t the $\mathbf{r}$-independent local values of the corresponding quantities at the point with the radius vector $\mathbf{r}_s(t)$, i.e., $n_v(\mathbf{r}_s)$ and $\mathbf{v}_v(\mathbf{r}_s)$. In view of what was said above, as an approximation correctly describing the shape of a 2D dark soliton in the case considered, it is natural to choose the function $\Phi_s(\mathbf{r}-\mathbf{r}_s(t),\dot{\mathbf{r}}_s(t))$ with time-dependent parameters. Using a simple algebra, $\Phi_s(\mathbf{r}-\mathbf{r}_s(t),\dot{\mathbf{r}}_s(t))$ can be expressed via the wave function $\bar{\Psi}_s(\bar{\xi},\bar{\eta},\bar{v})$ which we introduced before (see Sec. II C):

$$\Phi_s(\mathbf{r}-\mathbf{r}_s(t),\dot{\mathbf{r}}_s(t)) = \bar{\Psi}_s(\bar{\xi},\bar{\eta},\bar{v}(t)), \tag{19}$$

where

$$\bar{\xi} = \frac{1}{\bar{v}}(\mathbf{r}-\mathbf{r}_s)\cdot[\dot{\mathbf{r}}_s - \mathbf{v}_v(\mathbf{r}_s)], \tag{20}$$

$$\bar{\eta} = \frac{1}{\bar{v}}(\mathbf{r}-\mathbf{r}_s)\cdot\{\mathbf{z}_0\times[\dot{\mathbf{r}}_s - \mathbf{v}_v(\mathbf{r}_s)]\} \tag{21}$$

are the normalized orthogonal curvilinear coordinates that accompany a soliton along its propagation path, $\mathbf{z}_0$ is a single vector that is perpendicular to the x, y plane and is directed along the z axis, and the quantity

$$\bar{v}(t) = \bar{v}(\mathbf{r}_s(t),\dot{\mathbf{r}}_s(t)) = \frac{|\dot{\mathbf{r}}_s(t) - \mathbf{v}_v(\mathbf{r}_s(t))|}{\sqrt{n_v(\mathbf{r}_s(t))}} \tag{22}$$

has the meaning of the *normalized velocity* of a solitonlike structure in the coordinate system $\bar{\xi}$, $\bar{\eta}$.

Substitute into the Lagrange function density (18), instead of $\Phi(\mathbf{r},t)$, its approximation $\Phi_s(\mathbf{r}-\mathbf{r}_s(t),\dot{\mathbf{r}}_s(t))$, which, as was discussed above, locally describes well the shape of the solitary density drop moving in an inhomogeneous vortex flow of BEC at long distances from the center of a single topological defect. Taking into account the smooth dependence of the vector field $\mathbf{v}_v(\mathbf{r})$ and the background density $n_v(\mathbf{r})$ of the condensate on the coordinates $\mathbf{r}$ on characteristic scales Λ_s of the considered quasisoliton structure, and also assuming that the velocity $\dot{\mathbf{r}}_s(t)$ of a 2D dark soliton slowly varies in time, we proceed, in accordance with Eqs. (20) and (21) and using transformation of the rotation and additional normalization, to the new variables $\bar{\xi}$ and $\bar{\eta}$ and integrate $\mathcal{L}(\Phi_s,\Phi_s^*)$ over these variables. If we make use of the mirror symmetry of the function $\bar{\Psi}_s(\bar{\xi},\bar{\eta},\bar{v})$ with respect to $\bar{\eta}=0$, i.e., $\bar{\Psi}_s(\bar{\xi},\bar{\eta},\bar{v})=\bar{\Psi}_s(\bar{\xi},-\bar{\eta},\bar{v})$, asymptotic forms of its behavior on the infinity [33,34,40,41], and relations (13), we arrive at the following expression:

$$\bar{\mathcal{L}}(\mathbf{r}_s,\dot{\mathbf{r}}_s)=-\iint_{D_s}\mathcal{L}(\Phi_s(\tilde{\mathbf{r}},\dot{\mathbf{r}}_s(t)),\Phi_s^*(\tilde{\mathbf{r}},\dot{\mathbf{r}}_s(t)))\,d^2\tilde{\mathbf{r}}$$
$$=n_v(\mathbf{r}_s)[\bar{v}(\mathbf{r}_s,\dot{\mathbf{r}}_s)\bar{\mathcal{P}}(\bar{v}(\mathbf{r}_s,\dot{\mathbf{r}}_s))-\bar{\mathcal{E}}(\bar{v}(\mathbf{r}_s,\dot{\mathbf{r}}_s))]. \quad (23)$$

Here, $\tilde{\mathbf{r}}=\mathbf{r}-\mathbf{r}_s(t)$, D_s is the localization region of the soliton, and the quantities $\bar{\mathcal{P}}(\bar{v}(\mathbf{r}_s,\dot{\mathbf{r}}_s))$ and $\bar{\mathcal{E}}(\bar{v}(\mathbf{r}_s,\dot{\mathbf{r}}_s))$ at each fixed moment of time t are the corresponding integral characteristics of a 2D dark soliton, which in a flow-free homogeneous condensate of unit density could propagate along a straight line at a constant velocity equal to the value $\bar{v}(\mathbf{r}_s,\dot{\mathbf{r}}_s)$ calculated for a given t by Eq. (22). In what follows, by analogy with [40,41], we will call $\bar{\mathcal{P}}(\bar{v}(\mathbf{r}_s,\dot{\mathbf{r}}_s))$ and $\bar{\mathcal{E}}(\bar{v}(\mathbf{r}_s,\dot{\mathbf{r}}_s))$ the *normalized momentum* and *normalized energy* of the quasisoliton structure considered. The quantities $\bar{\mathcal{P}}(\bar{v}(\mathbf{r}_s,\dot{\mathbf{r}}_s))$ and $\bar{\mathcal{E}}(\bar{v}(\mathbf{r}_s,\dot{\mathbf{r}}_s))$ defined in such a way are connected to each other by the nonlinear dispersion relations (14) and (15).

Now, a 2D dark soliton can be interpreted as a quasiparticle with the *Lagrange function* (23). If at the times $t=t_1$ and t_2 this quasiparticle is located at certain points of space with the radius vectors $\mathbf{r}_{s1}=\mathbf{r}_s(t_1)$ and $\mathbf{r}_{s2}=\mathbf{r}_s(t_2)$, then between them it moves along the path on which the so-called *action functional*

$$\bar{\mathcal{I}}=\int_{t_1}^{t_2}\bar{\mathcal{L}}(\mathbf{r}_s(t),\dot{\mathbf{r}}_s(t))\,dt \quad (24)$$

takes an extreme value. This statement follows from the fact that the Lagrangian (23) was constructed directly on the basis of the Lagrange function density (18) of the exact equation (17) describing the dynamics of considered solitonlike structure in a smoothly inhomogeneous BEC (including that in the cloud of ultracold Bose gas with a single quantum vortex at the center). Varying the action functional (24) with respect to $\mathbf{r}_s(t)$ and $\dot{\mathbf{r}}_s(t)$ and using the condition of its extreme value on the true path of the soliton, we arrive at the Euler-Lagrange equation

$$\frac{d}{dt}\left[\frac{\partial\bar{\mathcal{L}}(\mathbf{r}_s,\dot{\mathbf{r}}_s)}{\partial\dot{\mathbf{r}}_s}\right]-\frac{\partial\bar{\mathcal{L}}(\mathbf{r}_s,\dot{\mathbf{r}}_s)}{\partial\mathbf{r}_s}=0\,, \quad (25)$$

which reduces to the following form:

$$\frac{d}{dt}\left\{\frac{\bar{\mathcal{P}}(\bar{v}(\mathbf{r}_s,\dot{\mathbf{r}}_s))}{\bar{v}(\mathbf{r}_s,\dot{\mathbf{r}}_s)}[\dot{\mathbf{r}}_s-\mathbf{v}_v(\mathbf{r}_s)]\right\}$$
$$+\left[\bar{\mathcal{E}}(\bar{v}(\mathbf{r}_s,\mathbf{v}_s))-\frac{1}{2}\bar{v}(\mathbf{r}_s,\mathbf{v}_s)\bar{\mathcal{P}}(\bar{v}(\mathbf{r}_s,\mathbf{v}_s))\right]\frac{\partial n_v(\mathbf{r}_s)}{\partial\mathbf{r}_s}$$
$$+\frac{\bar{\mathcal{P}}(\bar{v}(\mathbf{r}_s,\dot{\mathbf{r}}_s))}{\bar{v}(\mathbf{r}_s,\dot{\mathbf{r}}_s)}\left\{[\dot{\mathbf{r}}_s-\mathbf{v}_v(\mathbf{r}_s)]\cdot\frac{\partial}{\partial\mathbf{r}_s}\right\}\mathbf{v}_v(\mathbf{r}_s)=0. \quad (26)$$

Mathematically, relation (26) is a vector equation of the second order, which establishes the connection between the acceleration $\ddot{\mathbf{r}}_s(t)$ of a 2D dark soliton, its velocity $\dot{\mathbf{r}}_s(t)$, and the position of $\mathbf{r}_s(t)$ in space.

Using the *Hamiltonian formalism* developed in classical mechanics [90,91], by introducing as the vector of independent variables, instead of $\dot{\mathbf{r}}_s$, the *generalized momentum*

$$\mathbf{p}_s(\mathbf{r}_s,\dot{\mathbf{r}}_s)=\frac{\partial\bar{\mathcal{L}}(\mathbf{r}_s,\dot{\mathbf{r}}_s)}{\partial\dot{\mathbf{r}}_s}=\frac{\bar{\mathcal{P}}(\bar{v}(\mathbf{r}_s,\dot{\mathbf{r}}_s))}{\bar{v}(\mathbf{r}_s,\dot{\mathbf{r}}_s)}[\dot{\mathbf{r}}_s-\mathbf{v}_v(\mathbf{r}_s)] \quad (27)$$

we can pass from fairly cumbersome expression (26) to the so-called *canonic equations*, which are more convenient for analysis and numerical solution:

$$\frac{d\mathbf{r}_s}{dt}=\frac{\partial\bar{\mathcal{H}}(\mathbf{r}_s,\mathbf{p}_s)}{\partial\mathbf{p}_s}=\sqrt{n_v(\mathbf{r}_s)}\,\bar{v}(\bar{\mathcal{E}}(\mathbf{r}_s,\mathbf{p}_s))\frac{\mathbf{p}_s}{|\mathbf{p}_s|}+\mathbf{v}_v(\mathbf{r}_s), \quad (28)$$

$$\frac{d\mathbf{p}_s}{dt}=-\frac{\partial\bar{\mathcal{H}}(\mathbf{r}_s,\mathbf{p}_s)}{\partial\mathbf{r}_s}=-\left(\mathbf{p}_s\cdot\frac{\partial}{\partial\mathbf{r}_s}\right)\mathbf{v}_v(\mathbf{r}_s)$$
$$+\left[\frac{|\mathbf{p}_s|\bar{v}(\bar{\mathcal{E}}(\mathbf{r}_s,\mathbf{p}_s))}{2\sqrt{n_v(\mathbf{r}_s)}}-\bar{\mathcal{E}}(\mathbf{r}_s,\mathbf{p}_s)\right]\frac{\partial n_v(\mathbf{r}_s)}{\partial\mathbf{r}_s}, \quad (29)$$

where

$$\bar{\mathcal{H}}(\mathbf{r}_s,\mathbf{p}_s)=\mathbf{p}_s\cdot\dot{\mathbf{r}}_s(\mathbf{r}_s,\mathbf{p}_s)-\bar{\mathcal{L}}(\mathbf{r}_s,\dot{\mathbf{r}}_s(\mathbf{r}_s,\mathbf{p}_s))$$
$$=n_v(\mathbf{r}_s)\bar{\mathcal{E}}(\mathbf{r}_s,\mathbf{p}_s)+\mathbf{p}_s\cdot\mathbf{v}_v(\mathbf{r}_s) \quad (30)$$

is the *Hamiltonian* of a quasiparticle corresponding to the quasisoliton structure considered. Since this Hamiltonian does not depend explicitly on time, the conservation law

$$n_v(\mathbf{r}_s)\bar{\mathcal{E}}(\mathbf{r}_s,\mathbf{p}_s)+\mathbf{p}_s\cdot\mathbf{v}_v(\mathbf{r}_s)=H=\text{const} \quad (31)$$

will be fulfilled, according to which the normalized energy of a 2D dark soliton should vary along its propagation path as follows:

$$\bar{\mathcal{E}}(\mathbf{r}_s,\mathbf{p}_s)=\frac{H-\mathbf{p}_s\cdot\mathbf{v}_v(\mathbf{r}_s)}{n_v(\mathbf{r}_s)}, \quad (32)$$

where the constant H is determined by the initial conditions. Knowing $\bar{\mathcal{E}}$, one can also find the function $\bar{v}(\mathbf{r}_s,\mathbf{p}_s)$, using the chosen approximations (14) and (15) for the dependence $\bar{\mathcal{P}}(\bar{\mathcal{E}})$:

$$\bar{v}(\bar{\mathcal{E}}(\mathbf{r}_s,\mathbf{p}_s))=\left[\frac{d\bar{\mathcal{P}}}{d\bar{\mathcal{E}}}\right]^{-1}\Bigg|_{\bar{\mathcal{E}}(\mathbf{r}_s,\mathbf{p}_s)}. \quad (33)$$

As was mentioned in the Introduction, in Refs. [40,41] we analyzed in detail the case where in the background BEC there are no flows, and the stationary distribution of the condensate density $n_b(\mathbf{r})$ was formed under the action of an external potential $V_{ext}(\mathbf{r})$. If in relations (28) and (29) we set $\mathbf{v}_v(\mathbf{r})=0$ and $n_v(\mathbf{r})=n_b(\mathbf{r})$, where in the TF approximation $n_b(\mathbf{r})\approx 1-V_{ext}(\mathbf{r})>0$, then expressions (28) and (29) can

be transformed to the equations obtained in papers [40,41] for the propagation path of a 2D dark soliton in a flow-free inhomogeneous condensate with the undisturbed density $n_b(\mathbf{r})$. Derivation of the equations of motion, which is given in [40,41], is based not on the Whitham method, but on a rigorous asymptotic expansion using Fredholms alternative theorem [79,80]. This fact confirms the validity of the variational approach used here.

In the next section, we discuss scattering of 2D dark solitons by the inhomogeneities of the singular velocity field $\mathbf{v}_v(\mathbf{r}) = \boldsymbol{\varphi}_0/r$ created by a single quantum vortex and directed along the angular variable φ of the polar coordinate system r, φ and by the inhomogeneities of the axially symmetric distribution $n_v(r)$ of the BEC density. According to Sec. II B, in the absence of the external potential, i.e., in cases where the action of the external forces on the rarefied ultracold Bose gas is negligibly small in the space domain in the x, y plane the density $n_v(r)$ of the condensate is well described using the Padé approximation (7). If the effect of a large-scale trap $V_{ext}(r)$ where $1 - V_{ext}(r) > 0$ is taken into account, then for $n_v(r)$ one can use expression (9), which corresponds to the generalization of the TF approximation in the presence of a single topological defect at the BEC cloud center.

Taking into account that $\mathbf{v}_v(\mathbf{r}) = \boldsymbol{\varphi}_0/r$, and $n_v(\mathbf{r})$ depends only on the radial coordinate r, we rewrite expression (22) for the normalized velocity $\bar{v}(t)$ of a 2D dark soliton in the following way:

$$\bar{v}(t) = \bar{v}(r_s,\dot{r}_s,\dot{\varphi}_s) = \sqrt{\frac{r_s^2\dot{r}_s + \left(r_s^2\dot{\varphi}_s - 1\right)^2}{r_s^2 n_v(r_s)}}, \qquad (34)$$

where $r_s = r_s(t)$ and $\varphi_s = \varphi_s(t)$ is the position of the center of the solitonlike structure in the polar coordinate system r, φ connected with a single quantum vortex. The dots over the variables denote the derivatives with respect to time t. From relation (34) and equality $n_v(\mathbf{r}_s) = n_v(r_s)$ it follows directly that the Lagrangian (18) does not depend explicitly on the angular variable φ_s, i.e., for the quasiparticle associated with the solitary density drop considered, φ_s is a *cyclic* generalized coordinate. By virtue of the Lagrange equations, the generalized momentum $\ell_s = \partial\bar{\mathcal{L}}/\partial\dot{\varphi}_s$ corresponding to φ_s is the motion integral:

$$\frac{\bar{\mathcal{P}}(\bar{v}(r_s,\dot{r}_s,\dot{\varphi}_s))}{\bar{v}(r_s,\dot{r}_s,\dot{\varphi}_s)}\left(r_s^2\dot{\varphi}_s - 1\right) = M = \text{const}. \qquad (35)$$

This fact, together with the conservation law (31) rewritten in the form

$$n_v(r_s)\bar{\mathcal{E}}(\bar{v}(r_s,\dot{r}_s,\dot{\varphi}_s)) + \frac{M}{r_s^2} = H = \text{const}, \qquad (36)$$

significantly simplifies the solution of Eq. (26). With analytical approximations (14) and (15), for the dependence of the normalized momentum $\bar{\mathcal{P}}$ of a solitonlike structure on its normalized energy $\bar{\mathcal{E}}$ of relations (35) and (36) it is sufficient that the problem of the dynamics of a 2D dark soliton is reduced to the quadratures. In particular, using these relations we obtain a transcendental algebraic equation for the minimum distance $r_{s\min}$ by which, according to the concept developed above, the quasiparticle approaches to the topological defect located at the point with $r = 0$. Substituting expression (34) for $\bar{v}(r_s,\dot{r}_s,\dot{\varphi}_s)$ into Eqs. (35) and (36) and assuming $\dot{r}_s = 0$, we find that

$$r_{s\,\min}^2 n_v(r_{s\min})\bar{\mathcal{P}}^2(\bar{\mathcal{E}}(r_{s\min})) = M^2, \qquad (37)$$

$$\bar{\mathcal{E}}(r_{s\min}) = \frac{H r_{s\,\min}^2 - M}{r_{s\,\min}^2 n_v(r_{s\min})}. \qquad (38)$$

From this relation, taking into account Eqs. (14) and (15) and using standard numerical methods (e.g., Neuton-Raphson method) [92], it is easy to find the value $r_{s\min}$.

III. NUMERICAL SIMULATION OF INTERACTION OF 2D DARK SOLITONS WITH A SINGLE QUANTUM VORTEX IN THE BEC

A. Formulation of the problem of scattering of a 2D dark soliton by a single quantum vortex

The numerical simulation of the dynamics of 2D dark solitons (in particular, vortex pairs) interacting with the vortex flow was performed both within the framework of the asymptotic theory developed in Sec. II D and directly using the GP equation (1) for the wave function $\Psi(\mathbf{r},t)$ of the BEC. In the latter case, we employed parallel algorithms based on the splitting scheme with fast Fourier transform (FFT) and adapted to high-performance multiprocessor systems (see, e.g., [93–95]). The wave function $\Psi(\mathbf{r},t)$ was calculated in detail on discrete spatial grids with a large number of nodes $(2^{13} \times 2^{13})$, which first of all permitted us to estimate reliably the radiative losses which are discussed in Sec. III C. The numerical calculation required multiple modeling of the condensate dynamics for different initial parameters. Therefore, using the CUDA development tools of GPGPU applications [93,94], we created a software package for numerical solution of the GP equation (1), which requires modern graphical processor units (GPU) of NVIDIA company.

Assume that a single quantum vortex with topological charge $\varkappa = +1$ (for definiteness) and centered at the origin of the Cartesian coordinate system x, y be excited in the initially homogeneous condensate. Let a 2D dark soliton (this can be a vortex pair as well), which is characterized by the normalized velocity $\bar{v}_0$ and related normalized energy $\bar{\mathcal{E}}_0 = \bar{\mathcal{E}}_0(\bar{v}_0)$ and momentum $\bar{\mathcal{P}}_0 = \bar{\mathcal{P}}_0(\bar{v}_0)$, start from the point $x_0 < 0$, y_0 along the x axis at the time $t = 0$. For relatively large values $|x_0|$, i.e., when $|x_0| \gg 1$ (namely, for such abscissas x_0 and arbitrary ordinates y_0 of the start point it can be said that the considered solitonlike structure is initially distant from the quantum vortex), the pattern of interaction of solitons with a topological defect qualitatively ceases to depend x_0 and is mainly determined by the parameters $\bar{v}_0$ and y_0. Therefore, to be specific, we present and discuss the results of numerical calculations for a fixed value of $x_0 = -25.6$. Then, by analogy with the classical problem of scattering [90,91], we will call the coordinate y_0 an *impact distance* (or an *impact parameter*).

Based on the factorized representation used in section (16), in direct numerical simulation within the framework of the GP equation (1), the BEC wave function $\Psi(\mathbf{r},t)$ at the initial time $t = 0$ was specified in the form of the product

$$\Psi(x,y,t=0) = \Psi_v(x,y)\Phi_s(x - x_0, y - y_0, v_{s0}\mathbf{x}_0). \qquad (39)$$

Here, the first cofactor $\Psi_v(x,y)$ is the stationary wave function corresponding to a single quantum vortex. The amplitude $\psi_v(x,y)$ of the complex function $\Psi_v(x,y)$ [and therefore the nonuniform distribution of the density $n_v(x,y)$ of a background ultracold Bose gas] at each node of the spatial grid was calculated by solving Eq. (4) without any approximations. The second cofactor $\Phi_s(x-x_0,y-y_0,v_{s0}\mathbf{x}_0)$ in Eq. (39) describes the form of the 2D dark soliton, which starts from the point x_0, y_0 in the positive direction of the x axis with velocity equal to v_{s0} in absolute value. In order to correctly specify $\Phi_s(x-x_0,y-y_0,v_{s0}\mathbf{x}_0)$ on the elements of a discrete grid, we first calculated the function $\bar{\Psi}_s(\bar{\xi},\bar{\eta},\bar{v}_0)$ by numerically solving the stationary NLS equation (10) (see Refs. [33,34,37,42] for details) and then scaled by a factor of $\sqrt{n_v(x_0,y_0)}$ and rotated the coordinate system $\bar{\xi}$, $\bar{\eta}$ through an angle

$$\alpha = \arcsin[v_{vy}(x_0,y_0)/\sqrt{n_v(x_0,y_0)}\bar{v}_0], \tag{40}$$

where $v_{vy}(x_0,y_0)$ is the y-axis projection of the velocity vector $\mathbf{v}_v(x,y)$ of the vortex flow of BEC created by a topological defect at the center of the 2D dark soliton.

According to the variational approach we developed in Sec. II D, a solitonlike structure that is incident on the initially isolated phase singularity can be put into correspondence with a quasiparticle whose motion obeys the canonic equations (28) and (29) having two first integrals (35) and (36). In the case considered, the constants M and H in Eqs. (35) and (36) are determined by the following expressions:

$$M = -\frac{\bar{\mathcal{P}}_0}{\bar{v}_0}\left[y_0\sqrt{n_{v0}\bar{v}_0^2 - \frac{x_0^2}{\left(x_0^2+y_0^2\right)^2}} + \frac{x_0^2}{x_0^2+y_0^2}\right], \tag{41}$$

$$H = n_{v0}\bar{\mathcal{E}}_0 + \frac{M}{x_0^2+y_0^2}, \tag{42}$$

where $n_{v0} = n_v(x_0,y_0)$ is the density of the background BEC at the point with the coordinates x_0 and y_0, which can be calculated using the Padé approximation (7). We used this approximation for solution of the system of Hamiltonian equations (28) and (29), as well as in the theoretical analysis and interpretation of the results.

B. Flyby and exchange modes of scattering of a 2D dark soliton by a single quantum vortex

Figures 4–6 show the results of direct numerical simulation within the framework of the GP equation (1) of the dynamics of 2D dark solitons in a smoothly inhomogeneous vortex flow of BEC for different initial normalized velocities and impact distances: $\bar{v}_0 = 0.3$ and $y_0 = -16$ (Fig. 4), $\bar{v}_0 = 0.5$ and $y_0 = 12.8$ (Fig. 5), and $\bar{v}_0 = 0.7$ and $y_0 = -9.6$ (Fig. 6). Fragments (a)–(c) in these figures are snapshots of the spatial distribution of the density of an ultracold Bose gas, which follow one another at equal intervals Δt (the time interval Δt is specific for each example). The trajectories of quasiparticles calculated using a system of Hamiltonian equations (28) and (29) are shown by solid lines for comparison. It is clearly seen that the core of a single quantum vortex is virtually not shifted with respect to its initial position, and all of the time is localized near the origin of the Cartesian coordinate system x, y, while the solitonlike structure during scattering propagates

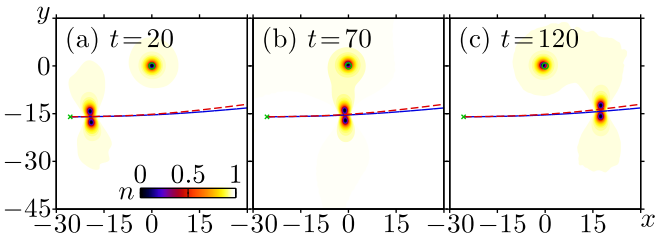

FIG. 4. (Color online) Snapshots of the BEC density at (a) $t = 20$, (b) $t = 70$, and (c) $t = 120$, which illustrate the process of scattering of a 2D dark soliton by a single quantum vortex (with a topological charge $\varkappa = +1$) excited in the initially homogeneous ultracold Bose gas and located at the origin of the Cartesian coordinate system x, y (unshaded green circle). At the time $t = 0$ the solitonlike structure starts from the point $x_0 = -25.6$, $y_0 = -16$ (green cross) in the positive direction of the x axis and has the normalized velocity $\bar{v}_0 = 0.3$, i.e., is initially a vortex pair. The condensate density distributions were obtained by direct numerical simulation performed immediately within the framework of the GP equation (1). The solid black line shows the trajectory of a composite quasiparticle, which is calculated using canonic equations (28) and (29). The dashed red line shows the trajectory of this quasiparticle, which is calculated in the small-angle approximation (53).

along the path which was found using the asymptotic theory developed in Sec. II D. Thus, with chosen values of $\bar{v}_0$ and y_0 the proposed variational approach adequately describes the behavior of a 2D dark soliton in a smoothly inhomogeneous vortex flow created in the BEC by a single phase singularity. However, we note for fairness sake that in all of the three cases the impact distance y_0 will be large enough in absolute value.

The numerical calculations performed directly within the framework of the GP equation (1) show that if the absolute value of the impact distance $|y_0|$ is decreased for a fixed start value of the normalized velocity $\bar{v}_0$, then sooner or later the situation will occur in which a 2D dark soliton moves strictly along the line obtained by using canonic equations (28) and (29) only at the initial stage (for a finite time) and then deviates from the given trajectory (see, e.g., Figs. 7 and 8). These figures demonstrate how a vortex pair with $\bar{v}_0 = 0.3$ that begins to move from two different points $x_0 = -25.6$, $y_0 = -4.8$ and $x_0 = -25.6$, $y_0 = 9.6$ is scattered by a single quantum vortex. Such a behavior is due to the fact that the solitonlike structure approaches the point $x = 0$, $y = 0$

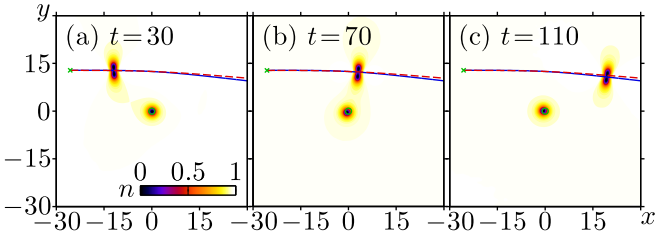

FIG. 5. (Color online) Same as Fig. 4, but at the times (a) $t = 30$, (b) $t = 70$, and (c) $t = 110$ for the 2D dark soliton which was initially specified in the form of a vortex pair with normalized velocity $\bar{v}_0 = 0.5$ and started from the point with the coordinates $x_0 = -25.6$ and $y_0 = 12.8$.

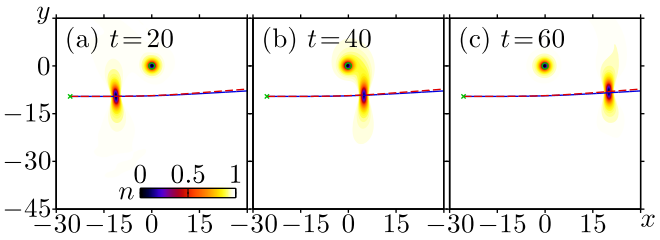

FIG. 6. (Color online) Same as Fig. 4, but at the times (a) $t = 20$, (b) $t = 40$, and (c) $t = 60$ for the initially vortex-free 2D dark soliton with normalized velocity $\bar{v}_0 = 0.7$ which started from the point with the coordinates $x_0 = -25.6$ and $y_0 = -9.6$.

(where the isolated topological defect was initially located) to a distance r_s, which is comparable with its characteristic size Λ_s. As a result, the conditions of applicability of the asymptotic theory developed in Sec. II D are violated, and the dynamics of a 2D dark soliton is subject to a variety of effects that were neglected when deriving a system of Hamiltonian equations (28) and (29). In particular, the motion of the center of a single quantum vortex and its final displacement with respect to the origin of the Cartesian coordinates x, y, and the emission of sound waves, as well as the disappearance and generation of zeros of the ultracold Bose gas density, with which the phase singularities of the BEC classical wave function are inseparably linked, were neglected.

Before proceeding to a more detailed discussion of the above processes, we emphasize that even in cases where the variational approach proposed in Sec. II D formally ceases to work, canonic equations (28) and (29) continue to be informative. First of all, it is shown that the change of the *flyby mode* of motion to the *mode of trapping* by the scattering center for the quasiparticles corresponding to the solitonlike structure is always indicative of a qualitative change in the

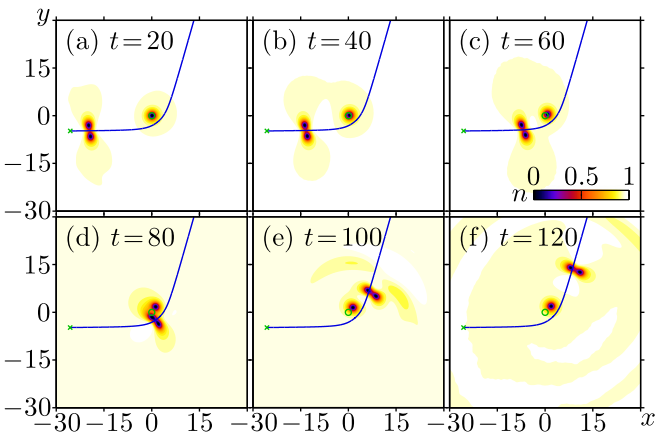

FIG. 7. (Color online) Same as Fig. 4, but at the times (a) $t = 20$, (b) $t = 40$, (c) $t = 60$, (d) $t = 80$, (e) $t = 100$, and (f) $t = 120$ for the 2D dark soliton, which is initially specified in the form of a vortex pair with the normalized velocity $\bar{v}_0 = 0.3$ and starts from the point $x_0 = -25.6$, $y_0 = -4.8$. The impact distance $y_0 = -4.8$ is smaller than the bifurcation value $y_{0a}(\bar{v}_0 = 0.3) \approx -3.44$, which corresponds to the flyby scattering mode of a solitonlike structure on a single quantum vortex.

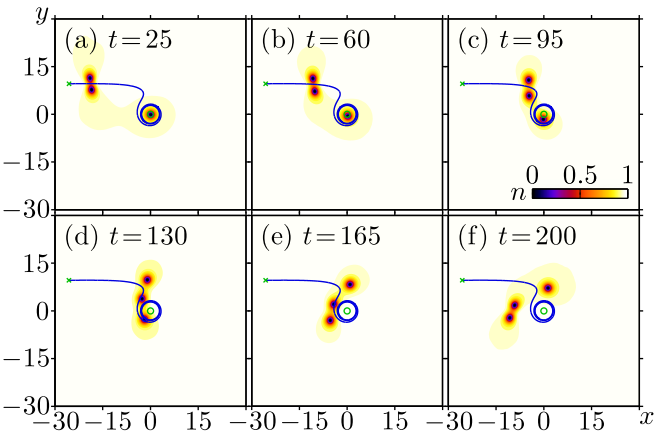

FIG. 8. (Color online) Same as Fig. 4, but at the times (a) $t = 25$, (b) $t = 60$, (c) $t = 95$, (d) $t = 130$, (e) $t = 165$, and (f) $t = 200$ for the 2D dark soliton, which is initially specified in the form of a vortex pair with the normalized velocity $\bar{v}_0 = 0.3$ and starts from the point $x_0 = -25.6$, $y_0 = 9.6$. The impact parameter $y_0 = 9.6$ lies in the interval $y_{0a} < y_0 < y_{0b}$, where $y_{0a}(\bar{v}_0 = 0.3) \approx -3.44$ and $y_{0b}(\bar{v}_0 = 0.3) \approx 13.65$, i.e., the exchange scattering mode of the solitonlike structure with a single quantum vortex is implemented.

nature of the interaction of 2D dark solitons with a single quantum vortex. Let us specify what we are speaking about.

With allowance for nonlinear dispersion relations (14) and (15) and Padé approximation (7) for the background condensate density $n_v(r)$, expressions (37) and (38) together with (41) and (42) are none other than a transcendental algebraic equation relative to $r_{s\min}$. From this equation, it is possible to find numerically the minimum distance $r_{s\min}$, to which the considered quasiparticle approaches the origin of the Cartesian coordinate system x, y, as a function of the impact parameter y_0 for fixed x_0 and $\bar{v}_0$. Figure 9 shows the dependencies $r_{s\min}(y_0)$ for the same abscissa $x_0 = -25.6$ of the start point of a 2D dark soliton and three values of its initial normalized velocity $\bar{v}_0$, namely, $\bar{v}_0 = 0.3$ (curve A), $\bar{v}_0 = 0.5$ (curve B), and $\bar{v}_0 = 0.7$ (curve C). The unshaded markers indicate the distances corresponding to the maximum approach of solitonlike structures with the initial position of a single quantum vortex. These distances were obtained by direct numerical simulation of the GP equation (1). That these markers fit well the corresponding diagrams $r_{s\min}(y_0)$ once again confirms the validity of the proposed method for describing the behavior of 2D dark solitons in a smoothly inhomogeneous BEC when stationary vortex flow is present in it. It is seen in Fig. 9 that for $y_0 \to \pm\infty$ the function $r_{s\min}(y_0)$ tends asymptotically to $|y_0|$, i.e., a 2D dark soliton moves almost along a straight line, irrespective of the presence of a single quantum vortex (which is quite natural). Comparing the curves A, B, and C in Fig. 9, it can easily be verified that, according to the asymptotic theory developed in Sec. II D, for a given impact parameter $y_0 = \text{const}$ the soliton with smaller initial normalized velocity $\bar{v}_0$ (and therefore greater initial normalized energy $\bar{\mathcal{E}}_0$ and momentum $\bar{\mathcal{P}}_0$) should come closer to the topological defect and, therefore, be more deflected from its initial propagation direction. In particular, this effect is also demonstrated by Figs. 10(a)–10(c), which were calculated using canonic equations (28) and (29) and show the proposed

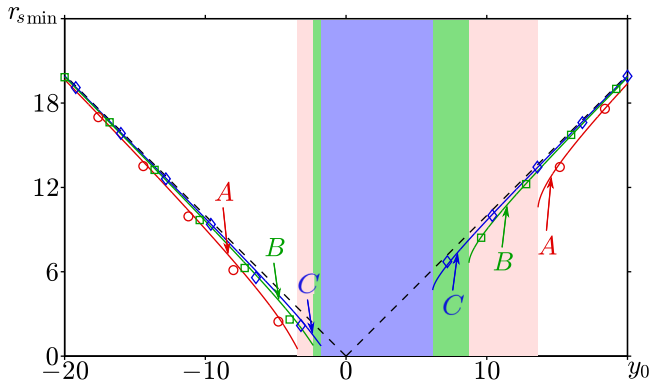

FIG. 9. (Color online) The dependencies of the minimum distances $r_{s\min}(y_0,\bar{v}_0)$ to which the quasiparticles starting from the points $x_0=-25.6$, y_0 and having different initial normalized velocities $\bar{v}_0$, namely, $\bar{v}_0=0.3$ (red solid curve A), $\bar{v}_0=0.5$ (green solid curve B), and $\bar{v}_0=0.7$ (blue solid curve C), approach the scattering center, which were calculated using the asymptotic theory developed in Sec. II D. For each value of $\bar{v}_0$ there is an interval from $y_{0a}(\bar{v}_0)$ to $y_{0b}(\bar{v}_0)$, inside which the transcendental algebraic equation connecting $r_{s\min}$ and impact parameters y_0 does not have real-valued solutions. These nested intervals correspond to the regions shown by colors of different shades. The contrast of these regions increases with increasing $\bar{v}_0$. Unshaded markers show the minimum distances to which the 2D dark solitons with $\bar{v}_0=0.3$ (red circles), $\bar{v}_0=0.5$ (green squares), and $\bar{v}_0=0.7$ (blue diamonds) approach the origin of the Cartesian coordinates x y, which were obtained by direct numerical calculations within the framework of the GP equation (1).

trajectories of motion of solitonlike structures according to $\bar{v}_0=0.3$, 0.5, and 0.7 for different y_0.

The transcendental algebraic equation connecting the minimum distance $r_{s\min}$ between the quasiparticle and the scattering center with the impact parameter y_0 does not have solutions in a certain, $\bar{v}_0$-dependent (as previously, x_0 is assumed fixed and equal to $x_0=-25.6$) interval of values

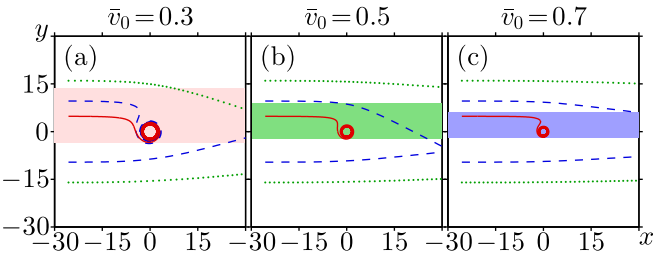

FIG. 10. (Color online) The trajectories of quasiparticles for three initial normalized velocities $\bar{v}_0$, namely, (a) $\bar{v}_0=0.3$, (b) $\bar{v}_0=0.5$, and (c) $\bar{v}_0=0.7$, which were calculated using canonic equations (28) and (29). The quasiparticles start in the positive direction of the x axis from the points $x_0=-25.6$, y_0, for which the impact distance y_0 takes the following values: $y_0=\pm16$ (green dotted lines), $y_0=\pm9.6$ (blue dashed lines), and $y_0=4.8$ (red solid line). If the impact parameter y_0 enters the interval $y_{0a}(\bar{v}_0)<y_0<y_{0b}(\bar{v}_0)$, to which its region shown by a color corresponds in each fragment (a), (b), or (c), then the quasiparticle is trapped by the scattering center located at the origin of the Cartesian coordinates x, y and approaches the scattering center by curling.

y_0, i.e., for $y_{0a}(\bar{v}_0)<y_0<y_{0b}(\bar{v}_0)$, where $y_{0a}(\bar{v}_0)<0$ and $y_{0b}(\bar{v}_0)>0$. This fact is clearly reflected in Fig. 9, in which it is seen how for $\bar{v}_0=$ const the diagram of the function $r_{s\min}(y_0)$ of the region of negative y_0 monotonically decreases, breaks at the point with $y_0=y_{0a}(\bar{v}_0)<0$, and then appears again for $y_0=y_{0b}(\bar{v}_0)>0$, continuously increasing with increasing y_0. We emphasize that the interval $y_{0a}(\bar{v}_0)<y_0<y_{0b}(\bar{v}_0)$ for any $\bar{v}_0$ is nonsymmetric with respect to $y_0=0$, and the inequality $y_{0b}(\bar{v}_0)>|y_{0a}(\bar{v}_0)|$ is always fulfilled, so that both $y_{0b}(\bar{v}_0)$ and $|y_{0a}(\bar{v}_0)|$ increase with decreasing initial normalized velocity $\bar{v}_0$ of a 2D dark soliton. The nested intervals from $y_{0a}(\bar{v}_0)$ to $y_{0b}(\bar{v}_0)$ for the same different $\bar{v}_0$ in Fig. 9 (and then in Figs. 10, 14, and 15) are shown by colors of different shades to improve visual perception.

The absence of solution in the transcendental algebraic equation for $r_{s\min}$ when $y_{0a}(\bar{v}_0)<y_0<y_{0b}(\bar{v}_0)$ is evidence for a bifurcation variation in the dynamic behavior of a quasiparticle for the impact distances $y_0=y_{0a}(\bar{v}_0)$ and $y_0=y_{0b}(\bar{v}_0)$. This is seen in Fig. 10 showing families of the trajectories of such quasiparticles, which were calculated using canonic equations (28) and (29). For $y_0\leqslant y_{0a}(\bar{v}_0)$ and $y_0\geqslant y_{0b}(\bar{v}_0)$ the quasiparticles can be called flyby since they go to infinity. If the start points lie inside the regions marked in Figs. 10(a)–10(c) by colors of different shades, i.e., the impact parameters y_0 enter the interval from $y_{0a}(\bar{v}_0)$ to $y_{0b}(\bar{v}_0)$, then the quasiparticles are trapped by the scattering center located at the origin of the Cartesian coordinates x, y and fall on it, performing curler motion.

The numerical calculations fulfilled directly within the framework of the GP equation (1) show that for $y_0\lesssim y_{0a}(\bar{v}_0)$ and $y_0\gtrsim y_{0b}(\bar{v}_0)$ the 2D dark solitons (in particular, vortex-antivortex pairs), which essentially are composite quasiparticles, as a result of scattering by a single quantum vortex are retained as an entity and indeed go to infinity, i.e., are flyby quasiparticles (see, e.g., Figs. 4–7). If $y_{0a}(\bar{v}_0)<y_0<y_{0b}(\bar{v}_0)$, then due to a collision with the core of the phase singularity, the initial (both vortical and vortex-free) 2D dark soliton is destroyed. One of its parts forms the core of a new single quantum vortex and another combines with the initially isolated topological defect and abandons the interaction region in the form of a newly generated solitonlike structure (see, e.g., Fig. 8). It can be said that the scattering is accompanied by a peculiar exchange, in which the current lines reconnect in the BEC [46–48]. Similar effects also occur in the analogous problem for three point vortices in hydrodynamics of incompressible fluid [50–52]. However, a specific feature of an ultracold Bose gas is its fundamental compressibility, due to which the considered processes are accompanied by radiative losses stipulated by the emission of sound waves [46–48].

Using the terminology proposed in [50], the first regime, in which the scattering is not followed by a break (in the sense mentioned above) of the solitonlike structure incident on the phase singularity, will be called a *flyby mode* and the second regime, an *exchange mode*. This terminology correlates in part with the classification of possible variants of the colliding particle interaction, which is adopted in nuclear physics [96].

Actually, the examples of flyby scattering of 2D dark solitons with different initial normalized velocities $\bar{v}_0$ for relatively large distances y_0 were given at the very beginning of this section (see Figs. 4–6). In this case, as was mentioned

above, a single quantum vortex remains almost fixed, and the behavior of a solitonlike structure is described with high accuracy within the framework of the variational approach proposed in Sec. II D.

Figure 7 demonstrates the process of flyby collision of a vortex pair ($\bar{v}_0 = 0.3$) with the initially isolated topological defect, in which the impact parameter $y_0 = -4.8$ is close enough to the bifurcation value $y_{0a}(\bar{v}_0 = 0.3) \approx -3.44$. At first [Figs. 7(a)–7(c)], such a pair moves with acceleration along the trajectory calculated using canonic equations (28) and (29). According to the developed theoretical concepts, when $y_0 < y_{0a}(\bar{v}_0)$ the velocity of a 2D dark soliton is the greater the smaller is the distance between the soliton and the center of the phase singularity. This is due mainly to two factors. First, the inhomogeneous vortex flow is oriented at an acute angle to the direction of motion of the solitonlike structure at each point of its propagation path. Second, as the distance between the isolated topological defect and the composite quasiparticles that is incident on it reduces, the normalized energy $\bar{\mathcal{E}}$ of the soliton decreases [see Eq. (36), where $2M > H$, $H > 0$], which unavoidably leads to an increase in the normalized velocity $\bar{v}$ and, as a consequence, variations in characteristic spatial sizes of a 2D dark soliton (we will come back to a discussion of this fact below when considering the small-angle scattering). In this case, when the vortex and antivortex (the zeros of the BEC density) in a pair converge as they approach the origin of the Cartesian coordinates x, y [see Figs. 7(b)–7(d)] and then diverge again as the solitonlike structure recedes to infinity [see Figs. 7(d)–7(f)]. When the vortex pair comes to the core of a single quantum vortex to a distance where the BEC flow created by the soliton in the region of localization of the core of the topological defect become significant, the center of the phase singularity begins to move and starts to shift from the point with the coordinates $x = 0$, $y = 0$ [see Figs. 7(c) and 7(d)]. After the end of the active-interaction stage, a single quantum vortex still remains shifted with respect to its initial position, which is seen in the Figs. 7(e) and 7(f). It is seen in these fragments how the sound waves are emitted during the collision of a vortex pair and a topological defect. Due to the effects mentioned above, a 2D dark soliton deviates from the trajectory predicted by canonic equations (28) and (29), in deriving which the dynamics of the center of a single quantum vortex and the radiative energy losses were neglected. As a result, the vortex pair propagates at a smaller angle to the x axis than was expected, and the distance between the zeros of the condensate density in a pair slightly reduces compared with the start instant for $t = 0$. Note that for $y_0 < y_{0a}(\bar{v}_0)$ during scattering the core of a single quantum vortex always remains closer to the vortex in the flyby solitonlike structure, and therefore the vortex pair during interaction with the initially isolated topological defect does not break.

The case where the initial normalized velocity $\bar{v}_0$ of the vortex pair that is incident on the phase singularity is close to the critical value $\bar{v}_* \approx 0.61$, upon exceeding which the vortex pair peels off circulation and becomes a vortex-free 2D dark soliton (see Sec. II C), is of particular interest. Such an example is shown in Fig. 11, where along with the snapshots of the BEC density distribution [Figs. 11(a)–11(c)], the phase structure of the condensate wave function [Figs. 11(d)–11(f)] is also

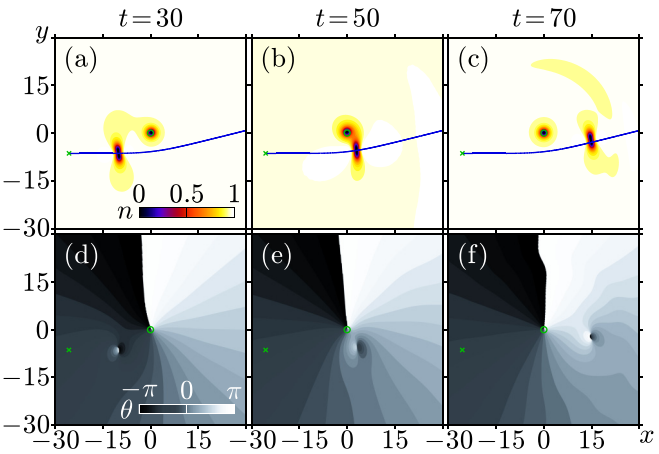

FIG. 11. (Color online) Snapshots (a)–(c) of the condensate density and (d)–(f) of the phase of the BEC wave function at the times (a), (d) $t = 30$, (b), (e) $t = 50$, and (c), (f) $t = 70$ for the case where a 2D dark soliton, which starts at $t = 0$ from the point $x_0 = -25.6$, $y_0 = -6.4$ (green cross) in the positive direction of the x axis and has the normalized velocity $\bar{v}_0 = 0.5$, i.e., initially represents a vortex pair, is incident on the initially isolated topological defect (with $\varkappa = +1$) located at the center of the Cartesian coordinate system x, y (unshaded green circle). Spatial distributions of the density and phase were obtained by direct numerical simulation performed immediately within the framework of the GP equation (1). A solid black curve shows the trajectory, which was calculated using canonic equations (28) and (29), of a composite quasiparticle corresponding to the solitonlike structure. In the active-interaction region [(b) and (e)] with single-phase singularity, the vortex pair transforms into a vortex-free soliton, which when moving away from the topological defect converts again into a vortex pair [(c) and (f)].

shown for clarity. In this case, the vortex pair with $\bar{v}_0 = 0.5$ begins to move from the point $x_0 = -25.6$, $y_0 = -6.4$ at $t = 0$ in the positive direction along the x axis. In the region of active interaction with the initially isolated topological defect, it transforms at first into a vortex-free 2D dark soliton [see Figs. 11(b) and 11(e)] and then transforms again into a vortex pair [see Figs. 11(c) and 11(f)]. This, in particular, is evidenced by the disappearance of 2π jumps in the wave-function phase in the soliton localization region on Fig. 11(e) and the appearance of these jumps again on Fig. 11(f). As was mentioned above, this behavior is due to a decrease in the normalized energy $\bar{\mathcal{E}}$ of a quasiparticle when $y_0 < y_{0a}(\bar{v}_0)$. On fragments (b) and (c) of Fig. 11 it is easily seen that the scattering is accompanied by the emission of sound waves. Radiation losses lead to a decrease in the normalized energy of the 2D dark soliton which escapes from the active-interaction region. However, in the discussed example, these losses are not sufficient that the incident vortex pair transforms into a vortex-free soliton due to a collision with the topological defect [see Figs. 11(c) and 11(f)].

Characteristic features of the exchange collisions of 2D dark solitons with a single quantum vortex are illustrated by Fig. 8. This figure shows snapshots of the BEC density for the case of scattering of a vortex pair that is incident on the initially isolated topological defect with the initial normalized velocity $\bar{v}_0 = 0.3$ under the impact distance $y_0 = 9.6 < y_{0b}(\bar{v}_0 = 0.3) \approx 13.65$. Figures 8(a)–8(c) clearly

demonstrate that at the initial stage, the vortex pair approaches the phase singularity, propagating along the path calculated using a system of Hamiltonian equations (28) and (29). When approaching a single quantum vortex, the 2D dark soliton is significantly slowed down, which results in changes in its characteristic spatial sizes. Specifically, the distance between the centers of the vortex and antivortex comprising the soliton increases. The considered composite quasiparticle is slowed down, first, due to an increase in its normalized energy $\bar{\mathcal{E}}$ as it approaches the origin of the Cartesian coordinate system x, y [see Eq. (36), where $2M < H$ and $H > 0$], and, second, by the vortex flow oriented at an obtuse angle to the direction of motion of the solitonlike structure at each point of its trajectory. Finally, the vortex pair ceases to exist as an entity and forms, by combining with the initially isolated topological defect, a system of three interacting objects, namely, two vortices and one antivortex [see Figs. 8(d) and 8(e)]. In this interaction, there is a fairly complex motion of the phase singularities (three zeros of the BEC density). At some instant, the distance between the centers of the antivortex and vortex that is initially at rest is smaller than the distance between the topological defects included in the 2D dark soliton at $t = 0$. Since the relation between two topological defects with azimuthal indices opposite in sign is determined by their relative position (the closer they are located, the stronger they are connected), the core of the vortex initially belonging to the incident vortex pair gradually stops and converts into the core of a stationary isolated topological defect shifted with respect to the origin of coordinates. In this case, the antivortex and the initially single quantum vortex form a new 2D dark soliton, which moves away from the point $x = 0$, $y = 0$ [see Fig. 8(f)]. It can be said that a new quasiparticle appears, which escapes the active-interaction region at an obtuse angle to the x axis, i.e., the so-called backscattering, which is typical of head-on collisions, takes place. As the case of flyby scattering, the exchange processes described here are accompanied by radiative losses stipulated by the emission of sound waves.

Figure 12 shows the dynamics of a vortex pair that is incident on the isolated topological defect with the initial normalized velocity $\bar{v}_0 = 0.5$ under the impact distance $y_0 = -0.8$ experiences an exchange collision with a single quantum vortex and, as a result, is scattered at an acute angle to the direction of its initial motion. It is seen on Figs. 12(a) and 12(b) that at the first stage, the 2D dark soliton moves almost along a straight line, gradually slowing down and rotating through a certain angle relative to the x axis, in full agreement with the theoretical concepts developed in Sec. II D. Then, the stage of active interaction of the vortex pair with a single-phase singularity comes [see Figs. 12(b)–12(e)]. In this case, the exchange processes follow the scenario described above. As a result, a new vortex pair and a new isolated topological defect are formed [see Fig. 12(f)]. It should be noted that in this situation, the radiative loss level is relatively low. Snapshots of the phase distribution of the BEC wave function give more detail to follow and get more information on how 2D dark solitons break and form. In particular, from fragments 12(g)–12(i) it can be concluded that the current lines reconnect at the time of the formation of a new vortex pair.

Figure 13 illustrates specific features of the exchange scattering of a vortex-free 2D dark soliton that is incident on

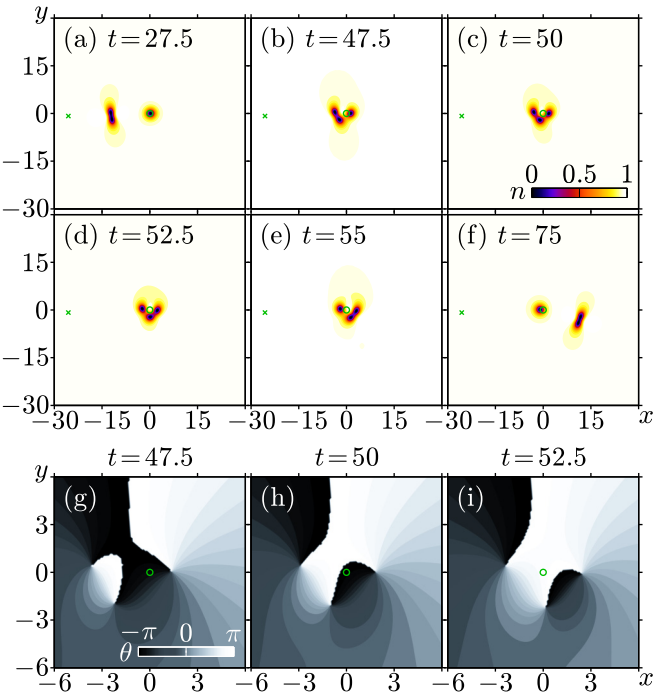

FIG. 12. (Color online) Snapshots (a)–(f) of the condensate density and (g)–(i) of the phase of the BEC wave function at the times (a) $t = 27.5$, (b), (g) $t = 47.5$, (c), (h) $t = 50$, (d), (i) $t = 52.5$, (e) $t = 55$, and (f) $t = 75$ for the case where a 2D dark soliton, which starts at $t = 0$ from the point $x_0 = -25.6$, $y_0 = -0.8$ (green cross) in the positive direction of the x axis and has the normalized velocity $\bar{v}_0 = 0.5$, i.e., is initially a vortex pair, is incident on the initially isolated topological defect (with $\varkappa = +1$) located at the origin of the Cartesian coordinate system x, y (unshaded green circle). Spatial distributions of the density and phase were obtained by direct numerical simulation performed immediately within the framework of the GP equation (1). The value of the impact parameter $y_0 = -0.8$ falls in the interval from $y_{0a}(\bar{v}_0 = 0.5) \approx -2.33$ to $y_{0b}(\bar{v}_0 = 0.5) \approx 8.74$. Therefore, the solitonlike structure has an exchange interaction with a single quantum vortex. This is demonstrated by (b)–(d) and (g)–(i). In this case, the radiative losses due to the sound-wave emission are small.

a single quantum vortex with the initial normalized velocity $\bar{v}_0 = 0.7$ under the impact distance $y_0 = -0.8$. As in the previous case, at the first stage the solitonlike structure propagates almost along a straight line because it is oriented in space so as to compensate for the drift along the y axis due to its own motion relative to the vortex flow. When approaching the initially isolated topological defect, the vortex-free 2D dark soliton is slowed down, and converts into a vortex pair when its normalized velocity becomes less than the critical value $\bar{v}_* \approx 0.61$ [see Figs. 13(b) and 13(g)]. It is exactly a pair that participates in the exchange process with a single quantum vortex following the scenario described above [see Figs. 13(b), 13(c), 13(g), and 13(h)], which results in that a new isolated topological defect appears and a new vortex pair is formed. After leaving the active-interaction region, the new vortex pair is accelerated and again converts into a vortex-free 2D dark soliton [see Figs. 13(c), 13(d), 13(h), and 13(i)]. Comparing Figs. 13(a) and 13(f), it can be noted that the

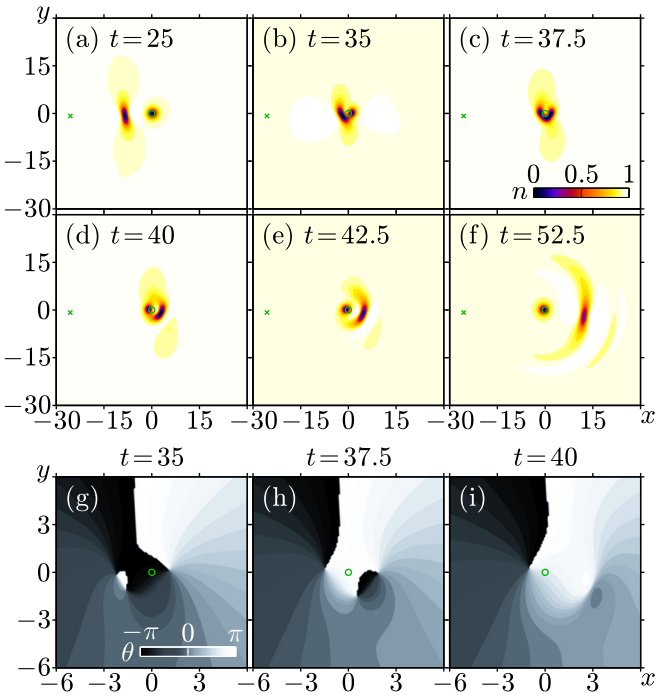

FIG. 13. (Color online) Same as Fig. 12, but at the times (a) $t = 25$, (b), (g) $t = 35$, (c), (h) $t = 37.5$, (d), (i) $t = 40$, (e) $t = 42.5$, and (f) $t = 52.5$ for the initially vortex-free 2D dark soliton with the normalized velocity $\bar{v}_0 = 0.7$. The value of the impact parameter $y_0 = -0.8$ falls in the interval from $y_{0a}(\bar{v}_0 = 0.7) \approx -1.77$ to $y_{0b}(\bar{v}_0 = 0.7) \approx 6.16$. Therefore, the exchange interaction mode takes place. In this case, the initially vortex-free solitonlike structure as it approaches the phase singularity converts at first into a vortex pair [(b) and (g)]. Then, the topological defect with $\varkappa = +1$, which is included in this pair, becomes isolated, so that the antivortex and the initially single quantum vortex form a new vortex pair [(c) and (h)], which later converts into a vortex-free 2D dark soliton [(d) and (i)]. Comparing (a) and (f), it can easily be verified that the new vortex-free solitonlike structure is a wider and less deep drop of the BEC density than the initial 2D dark soliton. This is due to the fairly intense emission of sound waves which can be noticed in (f).

vortex-free 2D dark soliton which formed after the collision is a wider and less deep density drop than the initial solitonlike structure which is incident on the single quantum vortex from the point $x_0 = -25.6$, $y_0 = -0.8$. First of all, this is due to significant radiative losses, which lead to a decrease in the normalized energy $\bar{\mathcal{E}}$. The emitted sound waves are distinctly seen in Fig. 13(f). Note that the radiative loss effect increases with increasing $\bar{v}_0$ (especially for the near-sound solitons, i.e., for $1 - \bar{v}_0 \ll 1$) since $\bar{\mathcal{E}}_0$ becomes comparable with unity in the dimensionless variables being used.

C. Radiative losses due to scattering of a 2D dark soliton by a single quantum vortex

We have repeatedly pointed out above that during interaction of a 2D dark soliton with a single quantum vortex, part of the energy stored in the solitonlike structure is emitted in the form of sound waves into the surrounding space. According to the theoretical concepts developed in Sec. II D, the value of the normalized energy $\bar{\mathcal{E}}_\infty^{\rm th}$ of a 2D dark soliton for $r_s \to \infty$ coincides with the constant H [see Eq. (36)], which, in turn, can be determined from the initial conditions at the start point x_0, y_0 from Eqs. (41) and (42). This statement is valid not only for flyby, but also exchange modes of scattering. If the emission of sound waves is neglected, then, by analogy with the problem on the behavior of three point vortices with the charges $\varkappa_1 = -\varkappa_2 = \varkappa_3 = +1$ in an ideal incompressible fluid, the new solitonlike structure (in particular, a vortex pair), irrespective of the dynamics of topological defects during the exchange collision, should also have the normalized energy $\bar{\mathcal{E}}_\infty^{\rm th}$ equal to H for $r_s \to \infty$. Therefore, as a qualitative characteristic of radiative losses, we have chosen the difference between $\bar{\mathcal{E}}_\infty^{\rm th} = H$ and the normalized energy $\bar{\mathcal{E}}_\infty^{\rm num}$ calculated by direct numerical simulation of the GP equation (1), which a 2D dark soliton has at very long distances $r_s \gg r_{s0} = \sqrt{x_0^2 + y_0^2}$ from the origin of the Cartesian coordinate system x, y after the scattering event by a single quantum vortex. The quantity $\bar{\mathcal{E}}_\infty^{\rm num}$ can be found by two methods. In one method, we first determine the stationary velocity $\bar{v}_\infty^{\rm num}$ of a solitary drop of the condensate density and, then, using the analytical approximation given by Eqs. (14) and (15) for $\bar{\mathcal{P}}(\bar{\mathcal{E}})$, we solve a transcendental algebraic equation. In another method, we calculate directly by the distribution of the BEC density $n(\mathbf{r},t)$ in the region of localization of a 2D dark soliton (see [40] for details).

Figure 14 shows the dependencies $\Delta\bar{\mathcal{E}} = \bar{\mathcal{E}}_\infty^{\rm th} - \bar{\mathcal{E}}_\infty^{\rm num}$ on the impact distance y_0 for three values of the initial normalized velocity $\bar{v}_0$, namely, $\bar{v}_0 = 0.3$ (solid red curve connecting unshaded red circles), $\bar{v}_0 = 0.5$ (solid green curve connecting unshaded green squares), and $\bar{v}_0 = 0.7$ (solid blue curve

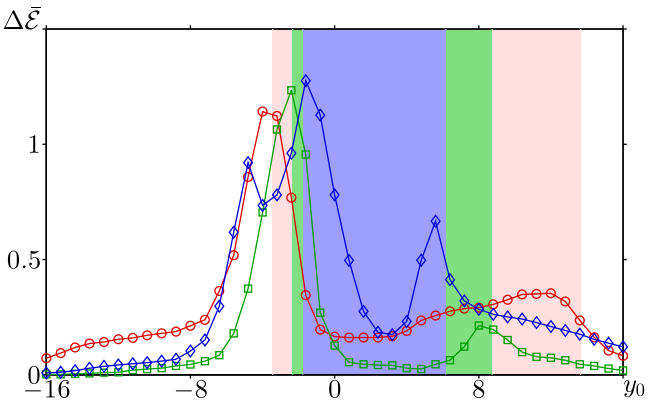

FIG. 14. (Color online) Dependencies of the radiative losses $\Delta\bar{\mathcal{E}}(y_0, \bar{v}_0)$ on the impact parameter y_0, which accompany the scattering by the initially single quantum vortex of 2D dark solitons that start in the positive direction of the x axis from the points with the coordinates $x_0 = -25.6$, y_0 and at the time $t = 0$ have different normalized velocities $\bar{v}_0$, namely, $\bar{v}_0 = 0.3$ (solid red curve connecting unshaded red circles), $\bar{v}_0 = 0.5$ (solid green curve connecting unshaded green squares), and $\bar{v}_0 = 0.7$ (solid blue curve connecting unshaded blue diamonds). For all three values of $\bar{v}_0$, the functions $\Delta\bar{\mathcal{E}}(y_0, \bar{v}_0)$ have local maxima near the boundaries $y_{0a}(\bar{v}_0)$ and $y_{0b}(\bar{v}_0)$ of the impact-parameter interval within which the solitonlike structure has an exchange interaction with the initially isolated topological defect. These nested intervals correspond to the regions shown by different-shade colors whose contrast increases with increasing $\bar{v}_0$.

connecting unshaded blue diamonds). It is seen that the function $\Delta\bar{\mathcal{E}}(y_0, \bar{v}_0 = \text{const})$ has pronounced maxima near the boundaries $y_0 = y_{0a}(\bar{v}_0)$ and $y_0 = y_{0b}(\bar{v}_0)$ which separate the regions of flyby and exchange interaction. In other words, the scattering of 2D dark solitons that are incident on a single quantum vortex under the impact distances y_0 close to the critical values $y_{0a}(\bar{v}_0)$ and $y_{0b}(\bar{v}_0)$ is accompanied by the most intense emission of sound waves. Such emission for $y_0 \approx y_{0b}(\bar{v}_0)$ is always smaller than for $y_0 \approx y_{0a}(\bar{v}_0)$. At the same time, in the interval $y_{0a}(\bar{v}_0) < y_0 < y_{0b}(\bar{v}_0)$ the radiative losses are markedly attenuated, and for large impact parameters y_0, when $|y_0| \gg y_b(\bar{v}_0)$, they become so small that they can generally be neglected. It should be mentioned that in the case of an initially vortex-free 2D dark soliton, when $\bar{v}_0 = 0.7$, the function $\Delta\bar{\mathcal{E}}(y_0)$ has one more additional local maximum lying on the left of the point $y_0 = y_{0a}(\bar{v}_0)$ (see Fig. 14, solid blue curve connecting unshaded blue diamonds).

The general features characteristic of all three dependencies $\Delta\bar{\mathcal{E}}(y_0, \bar{v}_0 = \text{const})$ presented in Fig. 14 can be explained by analyzing the accelerated motion of solitonlike structures along curved trajectories during their collision with a topological defect. Indeed, it is exactly the accelerated motion of localized drops of the density of an ultracold Bose gas that is directly related with the sound-wave emission: the greater the acceleration of the BEC density drops, the higher the intensity of the sound they emit [47]. A considerable increase in radiative losses in the vicinity of the negative bifurcation impact parameter $y_{0a}(\bar{v}_0)$ is due to the fact that for such y_0, the main changes in the velocity of a 2D dark soliton occur fairly rapidly within a small time span, while the soliton is located at distances comparable with its characteristic size Λ_s from the initially isolated phase singularity, i.e., in close vicinity of the core of the single quantum vortex. The longer the distance we go from the left boundary $y_{0a}(\bar{v}_0)$ into the interior of the impact-parameter interval $y_{0a}(\bar{v}_0) < y_0 < y_{0b}(\bar{v}_0)$, the greater the effect of the exchange processes on the dynamics of the BEC density drops. Essentially, these processes terminate the propagation path of a 2D dark soliton, and it has no time to reach the areas where, according to Eqs. (28) and (29), the soliton should undergo the maximum acceleration. As a result, the intensity of the emitted sound waves decreases. However, when the impact distance y_0 approaches its positive critical value $y_{0b}(\bar{v}_0)$, the radiative losses increase again. In the vicinity (somewhat left) of the point $y_0 = y_{0b}(\bar{v}_0)$ the function $\Delta\bar{\mathcal{E}}(y_0)$ reaches one more local maximum, whose appearance directly correlates with the fact that as it comes closer to the topological defect, the soliton is slowed down, its spatial sizes increase and, as a consequence, the scales of the exchange interaction region, from which the sound waves are emitted, also increase. Far from the boundaries of the interval $y_{0a}(\bar{v}_0) < y_0 < y_{0b}(\bar{v}_0)$, in the regions of large negative and positive parameters y_0 in absolute value, the sound-wave emission becomes very weak since the propagation paths of 2D dark solitons are gradual and the accelerations they experience are small. It will be shown in the next section that in this situation, it is possible to significantly simplify canonic equations (28) and (29), which describe the dynamics of solitonlike structures, and find an analytical expression for the scattering angle β in a way similar to that in classical mechanics for a particle that transits far enough from the center of the scattering potential [90,91].

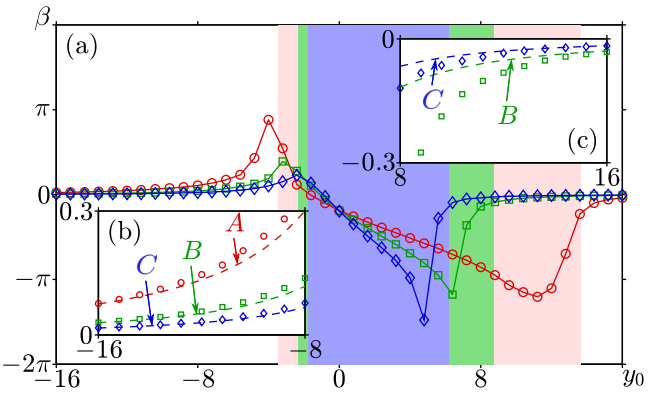

FIG. 15. (Color online) (a) Shows the dependencies of the angle $\beta(y_0, \bar{v}_0)$, to which a 2D dark soliton that starts from the points $x_0 = -26.6$, y_0 in the positive direction of the x axis with the initial normalized velocity $\bar{v}_0$ is scattered, on the impact distance y_0. The solid curves connecting the unshaded markers correspond to three different values of the initial normalized velocity $\bar{v}_0$ of a soliton: $\bar{v}_0 = 0.3$ (red curve connecting red circles), $\bar{v}_0 = 0.5$ (green curve connecting green squares), and $\bar{v}_0 = 0.7$ (blue curve connecting blue diamonds). The nested intervals $y_{0a}(\bar{v}_0) < y_0 < y_{0b}(\bar{v}_0)$ of the impact parameters y_0, for which the collisions of solitonlike structures with a solitary quantum vortex are exchange ones, correspond to the region indicated by different-shade colors, whose contrast increases with increasing $\bar{v}_0$. (b), (c) Include the parts illustrating the asymptotic behavior of the function $\beta(y_0, \bar{v}_0)$ for large negative and positive y_0, respectively. Here, the unshaded markers show the results obtained by direct numerical simulation immediately within the framework of the GP equation (1) and the dashed lines show the law determined by the analytical formula (54) for three different values $\bar{v}_0$: $\bar{v}_0 = 0.3$ (red curve A), $\bar{v}_0 = 0.5$ (green curve B), and $\bar{v}_0 = 0.7$ (blue curve C).

D. Small-angle approximation for scattering of 2D dark solitons by a single quantum vortex

Figure 15 shows the dependencies of the angles β of scattering of a 2D dark soliton by a single quantum vortex for three values of the initial normalized velocity $\bar{v}_0$, namely, $\bar{v}_0 = 0.3$ (solid red curve connecting unshaded red circles), $\bar{v}_0 = 0.5$ (solid curve connecting unshaded green square), and $\bar{v}_0 = 0.7$ (solid blue curve connecting unshaded blue diamonds) on the impact distance y_0. The angle β is reckoned from the x axis along the flow created in the BEC by an isolated topological defect (with the azimuthal index $\kappa = +1$), i.e., the positive β correspond to the counterclockwise rotation of the velocity vector $\dot{\mathbf{r}}_s(t)$ of a 2D dark soliton with respect to the initial direction. It is seen in Fig. 15 that the behavior of the functions $\beta(y_0, \bar{v}_0 = \text{const})$ is nonmonotonic. For example, if we move towards the point $y_0 = y_{0a}(\bar{v}_0)$ from the region of negative y_0, then the quantity β is always positive, and for a certain impact parameter smaller than $y_{0a}(\bar{v}_0)$ it reaches the maximum value $\beta_{\max}(\bar{v}_0)$. As the initial normalized velocity $\bar{v}_0$ decreases, the maximum scattering angle $\beta_{\max}(\bar{v}_0)$ increases; it can become greater than $\pi/2$ (as for $\bar{v}_0 = 0.3$) and approaches π in the limit $\bar{v}_0 \to 0$. Note that for $\beta = \pi$ the direction of motion of the solitonlike structure changes to strictly opposite,

i.e., the case of backscattering takes place. For each value $\bar{v}_0$ of those considered within the interval $y_{0a}(\bar{v}_0) < y_0 < y_{0b}(\bar{v}_0)$, where the collision of a 2D dark soliton with an isolated topological defect is an exchange one, the scattering β as a function of y_0 decays at first, vanishes, and goes to the region of negative values. When $\beta = 0$, the exchange interaction results in formation of a new (scattered) soliton moving in the same direction as the initial one. We also pay attention to the fact that the scattering angle $\beta(y_0 = 0, \bar{v}_0)$ corresponding to the zero impact distance $y_0 = 0$ does not depend on $\bar{v}_0$. For a certain value of the impact parameter y_0, which lies on the left of the point $y_0 = y_{0b}(\bar{v}_0)$, the function $\beta(y_0, \bar{v}_0 = \text{const})$ reaches its minimum $\beta_{\min}(\bar{v}_0) < -\pi$. This can be treated so that the solitonlike structure performs a clockwise rotation relative to its initial propagation direction through an angle exceeding π in absolute value. The further increase in y_0 is accompanied by an increase in the function $\beta(y_0, \bar{v}_0 = \text{const})$ and its gradual approach to zero from the side of the negative values.

Using the theoretical representations developed in Sec. II D, for each 2D dark soliton characterized by its initial normalized velocity $\bar{v}_0$, one can find the asymptotic forms of the function $\beta(y_0, \bar{v}_0 = \text{const})$ for large impact parameters y_0 in absolute value, when $\bar{v}_0|y_0| \gg 1$. This condition is certainly fulfilled for $|y_0| > y_{0b}(\bar{v}_0)$ since for any values of the initial normalized velocity $\bar{v}_0$, the product $\bar{v}_0 y_{0b}(\bar{v}_0)$ significantly exceeds unity. In this limiting case, the scattering of a 2D dark soliton is flyby and occurs at small angle $\beta \ll 1$. Let us analyze this situation in more detail.

First of all, we note that in the case considered, where $\bar{v}_0|y_0| \gg 1$, according to Eq. (36), the normalized energy $\bar{\mathcal{E}}$ of a 2D dark soliton along the trajectory of its motion undergoes only slight changes which, in the first order of smallness in $\epsilon = (\bar{v}_0|y_0|)^{-1} \ll 1$, are described by the following expression:

$$\bar{\mathcal{E}} \approx \bar{\mathcal{E}}_0 + \bar{\mathcal{P}}_0 y_0 / r_s^2 . \tag{43}$$

From Eq. (43) it is seen that if the impact parameter y_0 is negative, i.e., $y_0 < 0$, then as the solitonlike structure approaches the core of a single quantum vortex, the quantity $\bar{\mathcal{E}}$ slightly decreases, reaches its minimum value $\bar{\mathcal{E}}_{\min} \approx \bar{\mathcal{E}}_0 - \bar{\mathcal{P}}_0|y_0|/r_{s\min}^2$ when the distance r_s between the soliton and the topological defect is minimal, i.e., $r_s = r_{s\min}$, and then begins to increase with increasing r_s again. If the impact distance y_0 is positive, i.e., $y_0 > 0$, then during the propagation of a 2D dark soliton the quantity $\bar{\mathcal{E}}$ behaves in an opposite way, namely, it first increases up to $\bar{\mathcal{E}}_{\max} \approx \bar{\mathcal{E}}_0 + \bar{\mathcal{P}}_0|y_0|/r_{s\min}^2$ and then decreases to the initial value $\bar{\mathcal{E}}_0$.

It was mentioned above that knowing the behavior of the normalized energy $\bar{\mathcal{E}}$ of a 2D dark soliton along the trajectory of its motion, it is possible to describe the structural transformations occurring with it [40,41]. For example, according to the developed concepts for $y_0 < 0$, the process by which the configuration of a vortex pair is varied in the course of its scattering by a single quantum vortex is as follows. As the isolated topological defect is approached, the distance between the zeros of the BEC density in the pair decreases. If the initial normalized energies $\bar{\mathcal{E}}_0$ are such that $\bar{\mathcal{E}}_{\min} < \bar{\mathcal{E}}_*$, where $\bar{\mathcal{E}}_* \approx 7.59$ corresponds to the critical normalized velocity $\bar{v}_* \approx 0.61$, then the zeros of the condensate density completely disappear and the initially vortex 2D dark soliton becomes vortex free (literally speaking, the soliton peels off circulation). However, having escaped the region of interaction with the phase singularity, the solitonlike structure is reconstructed in the form of a vortex pair (if the weak emission of sound waves is neglected). The initially vortex-free 2D dark soliton, in which $\bar{v}_0 > \bar{v}_*$, and therefore $\bar{\mathcal{E}}_0 < \bar{\mathcal{E}}_*$, for $y_0 < 0$ still remains vortex free and only the depth of the density drop in it changes during the scattering. In the case where $y_0 > 0$, the vortex and antivortex comprising a vortex pair will diverge while $\bar{\mathcal{E}}$ increases. Once the value $\bar{\mathcal{E}}$ begins to decrease, the zeros of the condensate density in the pair will converse back, and the distance between them will recover (in the absence of radiative losses). In the case of a vortex-free soliton that starts from the point with $y_0 > 0$, the depth of the density drop in the solitonlike structure will increase when approaching the isolated topological defect, and then will decrease when moving away from the center of a single quantum vortex. If the initial normalized energy $\bar{\mathcal{E}}_0$ of the initially vortex-free 2D dark soliton ($\bar{\mathcal{E}}_0 < \bar{\mathcal{E}}_*$) takes such values that $\bar{\mathcal{E}}_{\max} > \bar{\mathcal{E}}_*$, then even in the course of its weak interaction with the phase singularity the soliton will convert into a vortex pair with two zeros of the BEC density and back.

To describe the small-angle scattering mode, we use canonic equations (28) and (29) and rewrite them as the x and y projections in the Cartesian coordinate system x, y connected with the center of a single quantum vortex. Expand the right-hand sides of the obtained relations in a series of powers of the small parameter ϵ, retaining only the number of terms required for finding the angle β:

$$\frac{dx_s}{dt} = \left[\bar{v}_0 + \frac{(\bar{w}_0\bar{\mathcal{P}}_0 - 1)y_0}{x_s^2 + y_s^2}\right]\frac{p_{sx}}{\bar{\mathcal{P}}_0} - \frac{y_s}{x_s^2 + y_s^2} + o(\epsilon^2), \tag{44}$$

$$\frac{dp_{sx}}{dt} = -\frac{2x_s y_s}{\left(x_s^2 + y_s^2\right)^2}\, p_{sx} + o(\epsilon^3), \tag{45}$$

$$\frac{dy_s}{dt} = \left[\bar{v}_0 + \frac{(\bar{w}_0\bar{\mathcal{P}}_0 - 1)y_0}{x_s^2 + y_s^2}\right]\frac{p_{sy}}{\bar{\mathcal{P}}_0} + \frac{x_s}{x_s^2 + y_s^2} + o(\epsilon^3), \tag{46}$$

$$\frac{dp_{sy}}{dt} = \frac{\left(x_s^2 - y_s^2\right)}{\left(x_s^2 + y_s^2\right)^2}\, p_{sx} + \frac{2x_s y_s}{\left(x_s^2 + y_s^2\right)^2}\, p_{sy} + \left(\frac{1}{2}\bar{v}_0\bar{\mathcal{P}}_0 - \bar{\mathcal{E}}_0\right)\frac{y_s}{\left(x_s^2 + y_s^2\right)^2} + o(\epsilon^4). \tag{47}$$

Here, the symbol $o(\epsilon^j)$ denotes the terms having the order ϵ^j or higher, and the constant $\bar{w}_0$ can easily be calculated using the approximations (14) and (15):

$$\bar{w}_0 = \left.\frac{d\bar{v}}{d\bar{\mathcal{E}}}\right|_{\bar{\mathcal{E}}=\bar{\mathcal{E}}_0} = \left.\frac{d^2\bar{\mathcal{P}}}{d\bar{\mathcal{E}}^2}\right|_{\bar{\mathcal{E}}=\bar{\mathcal{E}}_0}. \tag{48}$$

When writing these equations, we also took into account that the components of the vortex velocity field $\mathbf{v}_v(x, y)$ along the x and y directions at the point with the coordinates x_s and y_s have the values

$$v_{vx}(x_s, y_s) = -\frac{y_s}{x_s^2 + y_s^2}, \quad v_{vy}(x_s, y_s) = \frac{x_s}{x_s^2 + y_s^2}. \tag{49}$$

From Eqs. (44), (45), and (47) it follows immediately that

$$\frac{dx_s}{dt} = \bar{v}_0 + \frac{(\bar{w}_0\bar{\mathcal{P}}_0 - 1)y_0}{x_s^2 + y_s^2} + o(\epsilon^2), \tag{50}$$

$$p_{sx} = \bar{\mathcal{P}}_0 + \frac{\bar{\mathcal{P}}_0}{\bar{v}_0}\frac{y_s}{x_s^2 + y_s^2} + o(\epsilon^2), \tag{51}$$

$$p_{sy} = -\bar{\mathcal{P}}_0\frac{x_s}{x_s^2 + y_s^2} + o(\epsilon^2), \tag{52}$$

and according to Eqs. (46) and (52), the derivative $\dot{y}_s(t)$ has an order of smallness ϵ^2.

We now differentiate expression (46) over time t and make use of equality (47), retaining terms of the order of ϵ^2 and ϵ^3. The latter is not the exceeding of accuracy since $\ddot{y}_s(t) \sim \epsilon^3$. Finally, with allowance for Eq. (50), using the small-angle approximation, we obtain the following equation for the propagation path $y_s(x_s)$ of a 2D dark soliton (including a vortex pair) if a single quantum vortex is present in the BEC:

$$\frac{d^2y_s}{dx_s^2} = \frac{(\bar{w}_0\bar{\mathcal{P}}_0 - 1)}{\bar{v}_0^2}\frac{2y_0x_s^2}{\left(x_s^2 + y_s^2\right)^3} + \frac{\left(\bar{v}_0^2\bar{\mathcal{P}}_0 - 2\bar{v}_0\bar{\mathcal{E}}_0 - 2\bar{\mathcal{P}}_0\right)}{2\bar{v}_0^2}\frac{y_s}{\left(x_s^2 + y_s^2\right)^2}. \tag{53}$$

The dashed lines in Figs. 4–6 show the quasiparticle trajectories calculated in the small-angle approximation using Eq. (53). It is seen that they almost do not differ from the solutions of canonic equations (28) and (28) shown by solid lines.

Next, we proceed in the same way as in classical mechanics when deriving a formula for small deviation angles of the elementary particles scattered by a weak potential [90,91]. Let us integrate expression (53) over x_s, taking into account that in the integration-significant region where $x_s^2 \leqslant y_s^2$, the coordinate y_s differs only slightly from the impact distance y_0, i.e., assuming $y_s \approx y_0$. As a result, we find the low angle β, by which, according to the asymptotic theory developed, the solitonlike structure is scattered by an isolated topological defect:

$$\beta(y_0) = \frac{\pi\left(\bar{w}_0\bar{\mathcal{P}}_0^2 + 2\bar{v}_0^2\bar{\mathcal{P}}_0 - 3\bar{\mathcal{P}}_0 - 2\bar{v}_0\bar{\mathcal{E}}_0\right)}{4\bar{v}_0^2\bar{\mathcal{P}}_0}\frac{|y_0|}{y_0^3}. \tag{54}$$

Note that in this expression the factor enclosed in the parentheses is always negative for the parameters $\bar{\mathcal{E}}_0$, $\bar{\mathcal{P}}_0$, $\bar{v}_0$, and $\bar{w}_0$ corresponding to any 2D dark soliton from the discussed family of solitary structures. From Eq. (54) it is seen that for large absolute values of the impact distance y_0, where $|y_0| \gg \Lambda_s$, the scattering angle β decreases inversely proportionally to y_0^2. Also, according to Eq. (54), the angle β for a fixed value of $|y_0|$ is the greater, the smaller is the initial normalized velocity $\bar{v}_0$ (correspondingly the greater is the initial normalized energy $\bar{\mathcal{E}}_0$).

Figures 15(b) and 15(c) in clearly demonstrate that the dependencies $\beta(y_0, \bar{v}_0 = \text{const})$ constructed on the basis of the results of numerical calculations immediately within the framework of the GP equation (1) asymptotically reach the value determined by Eq. (54), which confirms that this formula is adequate.

Using Eq. (54) it is easy to find an expression for the linear differential cross section $\sigma(\beta)$:

$$\sigma(\beta) = -\frac{\sqrt{\pi\left(3 + 2\bar{v}_0\bar{\mathcal{E}}_0/\bar{\mathcal{P}}_0 - \bar{w}_0\bar{\mathcal{P}}_0 - 2\bar{v}_0^2\right)}}{4\bar{v}_0\beta^{3/2}}, \tag{55}$$

which is a complete analog of the well-known Rutherford formula for charged particles [90,91].

IV. CONCLUSIONS

Thus, within the framework of the mean-field approximation for the BEC with repulsive interaction between atoms, we have studied in detail the process of scattering of 2D dark solitons, and their vortex-antivortex pairs as a specific case, by a single quantum vortex excited in the initially homogeneous condensate. In the analysis of this problem, we used both analytical methods and direct numerical simulation by the GP equations (1) for the classical wave function. This problem is important and quite topical for the theory of coherent waves of matter and nonlinear wave processes in ultracold quantum gases. Sound waves, which have a Bogolyubov spectrum, and vortex-free 2D dark solitons can propagate in a BEC because of its compressibility and the presence of a specific quantum-mechanical pressure in it. These are essentially two main factors making the problem of scattering of 2D dark solitons by the initially isolated topological defect in the BEC different from the corresponding classical problem on the dynamics of three point vortices in an ideal incompressible fluid. To summarize, we briefly list the main results.

First, we have developed a variational approach to describe the dynamics of 2D dark solitons in a smoothly inhomogeneous BEC with a stationary flow inside. It has been shown that the solitonlike structures in such a condensate can be put into correspondence with quasiparticles, whose behavior obeys the canonic equations (28) and (29) of Hamiltonian mechanics.

Second, we have found two first integrals (35) and (36) of the system of Hamiltonian equations (28) and (29) with regard to scattering of a 2D soliton by a single quantum vortex in the presence of axial symmetry in the density distribution of the background condensate. This permitted us to propose a method for seeking the minimum distance $r_{s\min}$ to which a quasiparticle approaches the stationary scattering center and obtain a transcendental algebraic equation for $r_{s\min}$. This equation does not have real-valued solutions in the interval $y_{0a}(\bar{v}_0) < y_0 < y_{0b}(\bar{v}_0)$ of values of the impact parameter y_0, which depends on the initial normalized velocity $\bar{v}_0$ of a 2D dark soliton. The boundaries of this interval separate two possible modes of motion of quasiparticles, namely, flyby [when $y_0 \leqslant y_{0a}(\bar{v}_0)$ and $y_0 \geqslant y_{0b}(\bar{v}_0)$] and trapped [when $y_{0a}(\bar{v}_0) < y_0 < y_{0b}(\bar{v}_0)$].

Third, directly within the framework of the GP equation (1), we have performed a numerical simulation of the dynamics of the wave function of BEC, which permitted us to analyze in detail the scattering of 2D dark solitons by a single quantum vortex and explain all the key features and subtleties of the process using the theoretical concept we developed. In particular, it has been clearly demonstrated that the trajectories of motion and structural changes of the solitonlike structures are described with high accuracy using the proposed variational

approach for the impact distances y_0 significantly exceeding the characteristic spatial sizes of the soliton in absolute value. However, even in cases where the conditions of applicability of the analytical methods being used are violated and the asymptotic theory formally ceases to work, its results are still informative. Direct numerical calculations using the GP equation (1) show that for a fixed initial normalized velocity $\bar{v}_0$, change of the flyby mode of motion to the mode of trapping by the scattering center for the quasiparticles associated with the considered solitary drops of the condensate density, always indicates a qualitative change in the nature of the interaction of 2D dark solitons with the initially isolated topological defect. The bifurcation values $y_{0_a}(\bar{v}_0)$ and $y_{0_b}(\bar{v}_0)$ actually separate the radically different flyby and exchange collisions of solitonlike structures with phase singularity. In the case of flyby scattering [where $y_0 \lesssim y_{0_a}(\bar{v}_0)$ and $y_0 \gtrsim y_{0_b}(\bar{v}_0)$], both the vortex and vortex-free 2D dark solitons are retained as an entity throughout the entire path of its propagation and experience only internal structural transformations on the path. In the case of exchange interaction [where $y_{0_a}(\bar{v}_0) < y_0 < y_{0_b}(\bar{v}_0)$] of the initially vortex pairs ($\bar{v}_0 < \bar{v}_* \approx 0.61$) with a single quantum vortex, all the three topological defects come fairly close to each other and form a system of three equal actively contacting objects. There is complex motion of the phase singularities (zeros of the BEC density), which results in that the topological defects with azimuthal indices of the same sign change roles: the core of the initially moving vortex stops gradually and becomes the core of a stationary phase singularity, while the antivortex and the vortex that is initially at rest form a new pair that escapes from the strong interaction region to infinity. For vortex-free 2D dark solitons, the exchange interactions with an isolated topological defect follow a similar but more intriguing scenario. Such a soliton, as it approaches the topological defect, transforms into a vortex pair that participates in the exchange interaction with a single quantum vortex, which was described above. Finally, a new vortex pair forms, which is then accelerated, peels off circulation, and transforms into a vortex-free soliton.

Fourth, we have analyzed the radiative losses related to the sound-wave emission. It is shown that their intensity depends nonmonotonically on the impact distance y_0, under which a 2D dark soliton is incident on the topological defect, and reaches its maximum values near the critical values $y_{0_a}(\bar{v}_0)$ and $y_{0_b}(\bar{v}_0)$, where there is a change of the flyby and exchange collision modes.

Fifth, we have constructed the dependence of the scattering angle β of a 2D dark soliton on the impact distances y_0, which were obtained by numerically solving the GP equation (1). Using a small-angle approximation, we found analytical expressions connecting the scattering angle β and the linear differential cross section σ with the impact parameter y_0 and initial normalized velocity $\bar{v}_0$ of the solitonlike structure.

To conclude, we note that the inhomogeneity of most of the real BEC, which are confined (not only along the z axis, but also in the x, y plane) in the external trap $V_{ext}(\mathbf{r})$, can change dramatically the pattern of scattering of 2D dark solitons by a single quantum vortex. However, if the potential $V_{ext}(\mathbf{r})$ is wide and is axially symmetric, i.e., $V_{ext}(\mathbf{r}) = V_{ext}(r)$, and the isolated defect is initially located at the center, then the dynamics of a 2D dark soliton in such a smoothly inhomogeneous condensate with vortex flow can also be studied using the variational approach we developed here.

ACKNOWLEDGMENTS

The authors thank V. A. Mironov and J. J. Rasmussen for helpful discussions at the initial stage of this work. This work was supported by the Russian Science Foundation under Project No. 14-12-00811.

[1] A. L. Fetter, Rev. Mod. Phys. **81**, 647 (2009).
[2] R. Numasato, M. Tsubota, and V. S. L'vov, Phys. Rev. A **81**, 063630(12) (2010).
[3] B. Nowak, D. Sexty, and T. Gasenzer, Phys. Rev. B **84**, 020506 (2011).
[4] J. Schole, B. Nowak, and T. Gasenzer, Phys. Rev. A **86**, 013624 (2012).
[5] B. Nowak, J. Schole, D. Sexty, and T. Gasenzer, Phys. Rev. A **85**, 043627 (2012).
[6] T. Simula, M. J. Davis, and K. Helmerson, Phys. Rev. Lett. **113**, 165302 (2014).
[7] A. C. White, B. P. Anderson, and V. S. Bagnato, Proc. Natl. Acad. Sci. USA **111**, 4719 (2014).
[8] T. W. Neely, A. S. Bradley, E. C. Samson, S. J. Rooney, E. M. Wright, K. J. H. Law, R. Carretero-González, P. G. Kevrekidis, M. J. Davis, and B. P. Anderson, Phys. Rev. Lett. **111**, 235301 (2013).
[9] B. P. Anderson, J. Low Temp. Phys. **161**, 574 (2010).
[10] K. E. Wilson, E. C. Samson, Z. L. Newman, T. W. Neely, and B. P. Anderson, Annu. Rev. Cold Atoms Mol. **1**, 261 (2013).
[11] M. T. Reeves, B. P. Anderson, and A. S. Bradley, Phys. Rev. A **86**, 053621 (2012).
[12] A. S. Bradley and B. P. Anderson, Phys. Rev. X **2**, 041001 (2012).
[13] M. T. Reeves, T. P. Billam, B. P. Anderson, and A. S. Bradley, Phys. Rev. Lett. **110**, 104501 (2013).
[14] W. J. Kwon, G. Moon, J. Y. Choi, S. W. Seo, and Y. I. Shin, Phys. Rev. A **90**, 063627 (2014).
[15] G. W. Stagg, A. J. Allen, N. G. Parker, and C. F. Barenghi, Phys. Rev. A **91**, 013612 (2015).
[16] A. L. Fetter, J. Low Temp. Phys. **161**, 445 (2010).
[17] P. J. Torres, P. G. Kevrekidis, D. J. Frantzeskakis, R. Carretero-González, P. Schmelcher, and D. S. Hall, Phys. Lett. A **375**, 3044 (2011).
[18] P. J. Torres, R. Carretero-González, S. Middelkamp, P. Schmelcher, D. J. Frantzeskakis, and P. G. Kevrekidis, Commun. Pure Appl. Anal. **10**, 1589 (2011).
[19] S. Middelkamp, P. J. Torres, P. G. Kevrekidis, D. J. Frantzeskakis, R. Carretero-González, P. Schmelcher, D. V. Freilich, and D. S. Hall, Phys. Rev. A **84**, 011605 (2011).
[20] R. Navarro, R. Carretero-González, P. J. Torres, P. G. Kevrekidis, D. J. Frantzeskakis, M. W. Ray, E. Altuntaş, and D. S. Hall, Phys. Rev. Lett. **110**, 225301 (2013).

[21] V. Koukouloyannis, G. Voyatzis, and P. G. Kevrekidis, Phys. Rev. E **89**, 042905 (2014).

[22] D. Yan, R. Carretero-González, D. J. Frantzeskakis, P. G. Kevrekidis, N. P. Proukakis, and D. Spirn, Phys. Rev. A **89**, 043613 (2014).

[23] A. Lucas and P. Surówka, Phys. Rev. A **90**, 053617 (2014).

[24] T. P. Billam, M. T. Reeves, B. P. Anderson, and A. S. Bradley, Phys. Rev. Lett. **112**, 145301 (2014).

[25] T. P. Billam, M. T. Reeves, and A. S. Bradley, Phys. Rev. A **91**, 023615 (2015).

[26] V. A. Mironov, A. I. Smirnov, and L. A. Smirnov, J. Exp. Theor. Phys. **110**, 877 (2010), and references therein.

[27] V. A. Mironov, A. I. Smirnov, and L. A. Smirnov, J. Exp. Theor. Phys. **112**, 46 (2011), and references therein.

[28] L. A. Smirnov, D. A. Smirnova, E. A. Ostrovskaya, and Y. S. Kivshar, Phys. Rev. B **89**, 235310 (2014).

[29] Z. Dutton, M. Budde, C. Slowe, and L. V. Hau, Science **293**, 663 (2001).

[30] J. J. Chang, P. Engels, and M. A. Hoefer, Phys. Rev. Lett. **101**, 170404 (2008).

[31] M. A. Hoefer and B. Ilan, Phys. Rev. A **80**, 061601 (2009).

[32] F. Pinsker, N. G. Berloff, and V. M. Pérez-García, Phys. Rev. A **87**, 053624 (2013).

[33] C. A. Jones and P. H. Roberts, J. Phys. A: Math. Gen. **15**, 2599 (1982).

[34] C. A. Jones, S. J. Putterman, and P. H. Roberts, J. Phys. A: Math. Gen. **19**, 2991 (1986).

[35] E. A. Kuznetsov and J. J. Rasmussen, Phys. Rev. E **51**, 4479 (1995).

[36] N. G. Berloff and P. H. Roberts, J. Phys. A: Math. Gen. **37**, 11333 (2004).

[37] N. G. Berloff, J. Phys. A: Math. Gen. **37**, 1617 (2004).

[38] S. Tsuchiya, F. Dalfovo, C. Tozzo, and L. Pitaevskii, J. Low Temp. Phys. **148**, 393 (2007).

[39] S. Tsuchiya, F. Dalfovo, and L. Pitaevskii, Phys. Rev. A **77**, 045601 (2008).

[40] L. A. Smirnov and V. A. Mironov, Phys. Rev. A **85**, 053620 (2012), and references therein.

[41] V. A. Mironov and L. A. Smirnov, JETP Lett. **95**, 549 (2012).

[42] A. Paredes, D. Feijoo, and H. Michinel, Phys. Rev. Lett. **112**, 173901 (2014).

[43] L. P. Pitaevskii and S. Stringari, *Bose-Einstein Condensation*, 2nd ed. (Clarendon, Oxford, UK, 2003).

[44] C. Pethick and H. Smith, *Bose-Einstein Condensation in Dilute Gases*, 2nd ed. (Cambridge University Press, Cambridge, UK, 2008).

[45] P. G. Kevrekidis, D. J. Frantzeskakis, and R. Carretero-González, *Emergent Nonlinear Phenomena in Bose-Einstein Condensates: Theory and Experiment* (Springer, Berlin, 2008).

[46] N. G. Parker, Ph.D. thesis, Department of Physics, University of Durham, UK, 2004.

[47] C. F. Barenghi, N. G. Parker, N. P. Proukakis, and C. S. Adams, J. Low Temp. Phys. **138**, 629 (2005).

[48] N. G. Berloff, Phys. Rev. A **69**, 053601 (2004).

[49] H. Poincaré, in *Theorié des Tourbillons*, edited by G. Carré (Cours de la Faculté des Sciences de Paris, Paris, 1893).

[50] H. Aref, Phys. Fluids **22**, 393 (1979).

[51] W. Gröbli, Ph.D. thesis, Zürich: Zürcher und Furrer, 1877 [also published in Vierteljahrschriftder naturforschenden Gesellschaft in Zürich **22**, 37–81, 129–165 (1877)].

[52] H. Aref, N. Rott, and H. Thomann, Annu. Rev. Fluid Mech. **24**, 1 (1992).

[53] C. Nore, M. E. Brachet, E. Cerda, and E. Tirapegui, Phys. Rev. Lett. **72**, 2593 (1994).

[54] C. Wexler and D. J. Thouless, Phys. Rev. B **58**, R8897 (1998).

[55] S. G. Llewellyn Smith, J. Phys. A: Math. Gen. **35**, 3597 (2002).

[56] P. Capuzzi, F. Federici, and M. P. Tosi, Phys. Rev. A **78**, 023604 (2008).

[57] Y. Guo and O. Bühler, Phys. Fluids **26**, 027105 (2014).

[58] Y. S. Kivshar, A. Nepomnyashchy, V. Tikhonenko, J. Christou, and B. Luther-Davies, Opt. Lett. **25**, 123 (2000).

[59] D. Neshev, A. Nepomnyashchy, and Y. S. Kivshar, Phys. Rev. Lett. **87**, 043901 (2001).

[60] Y. V. Kartashov and A. M. Kamchatnov, Phys. Rev. A **89**, 055804 (2014).

[61] A. L. Gaunt, T. F. Schmidutz, I. Gotlibovych, R. P. Smith, and Z. Hadzibabic, Phys. Rev. Lett. **110**, 200406 (2013).

[62] T. F. Schmidutz, I. Gotlibovych, A. L. Gaunt, R. P. Smith, N. Navon, and Z. Hadzibabic, Phys. Rev. Lett. **112**, 040403 (2014).

[63] I. Gotlibovych, T. F. Schmidutz, A. L. Gaunt, N. Navon, R. P. Smith, and Z. Hadzibabic, Phys. Rev. A **89**, 061604 (2014).

[64] I. Aranson and V. Steinberg, Phys. Rev. B **53**, 75 (1996).

[65] P. Kuopanportti, E. Lundh, J. A. M. Huhtamäki, V. Pietilä, and M. Möttönen, Phys. Rev. A **81**, 023603 (2010).

[66] P. Kuopanportti and M. Möttönen, Phys. Rev. A **81**, 033627 (2010).

[67] C. Rorai, K. R. Sreenivasan, and M. E. Fisher, Phys. Rev. B **88**, 134522 (2013).

[68] F. Dalfovo and S. Stringari, Phys. Rev. A **53**, 2477 (1996).

[69] E. Lundh, C. J. Pethick, and H. Smith, Phys. Rev. A **55**, 2126 (1997).

[70] B. Jackson, J. F. McCann, and C. S. Adams, Phys. Rev. A **61**, 013604 (1999).

[71] A. A. Svidzinsky and A. L. Fetter, Phys. Rev. Lett. **84**, 5919 (2000).

[72] S. Middelkamp, P. G. Kevrekidis, D. J. Frantzeskakis, R. Carretero-González, and P. Schmelcher, Phys. Rev. A **82**, 013646 (2010).

[73] S. Middelkamp, P. G. Kevrekidis, D. J. Frantzeskakis, R. Carretero-González, and P. Schmelcher, J. Phys. B: At., Mol. Opt. Phys. **43**, 155303 (2010).

[74] B. P. Anderson, P. C. Haljan, C. E. Wieman, and E. A. Cornell, Phys. Rev. Lett. **85**, 2857 (2000).

[75] D. V. Freilich, D. M. Bianchi, A. M. Kaufman, T. K. Langin, and D. S. Hall, Science **329**, 1182 (2010).

[76] V. E. Zakharov and E. A. Kuznetsov, Phys. D (Amsterdam) **18**, 455 (1986).

[77] M. J. Ablowitz and P. A. Clarkson, *Solitons, Nonlinear Evolution Equations and Inverse Scattering* (Cambridge University Press, Cambridge, UK, 1991).

[78] E. Infeld and G. Rowlands, *Nonlinear Waves, Solitons and Chaos*, 2nd ed. (Cambridge University Press, Cambridge, UK, 2000).

[79] A. Scott, *Nonlinear Science: Emergence and Dynamics of Coherent Structures*, 2nd ed., Oxford Texts in Applied and Engineering Mathematics (Oxford University Press, Oxford, UK, 2003).

[80] Y. Kivshar and G. Agrawal, *Optical Solitons: From Fibers to Photonic Crystals* (Academic Press, Amsterdam, 2003).

[81] G. B. Whitham, *Linear and Nonlinear Waves*, reprint ed. (Wiley, New York, 1999).
[82] Y. S. Kivshar and W. Królikowski, Opt. Commun. **114**, 353 (1994).
[83] J. H. P. Dawes and H. Susanto, Phys. Rev. E **87**, 063202 (2013).
[84] D. Yan, P. G. Kevrekidis, and D. J. Frantzeskakis, J. Phys. A: Math. Theor. **44**, 415202 (2011).
[85] Q. Kong, Q. Wang, O. Bang, and W. Krolikowski, Phys. Rev. A **82**, 013826 (2010).
[86] S. Pu, C. Hou, K. Zhan, C. Yuan, and Y. Du, Opt. Commun. **285**, 3631 (2012).
[87] G. Theocharis, P. Schmelcher, M. K. Oberthaler, P. G. Kevrekidis, and D. J. Frantzeskakis, Phys. Rev. A **72**, 023609 (2005).
[88] E. A. Kuznetsov and S. K. Turitsyn, Zh. Eksp. Teor. Fiz. **94**, 119 (1988) [Sov. Phys. JETP **67**, 1583 (1988)].
[89] D. E. Pelinovsky and Y. S. Kivshar, Phys. Rep. **331**, 117 (2000).
[90] L. D. Landau and E. M. Lifshitz, *Mechanics*, 3rd ed. (Pergamon, Oxford, UK, 1976).
[91] H. Goldstein, *Classical Mechanics*, 2nd ed. (Addison-Wesley, Reading, MA, 1980).
[92] W. H. Press, S. A. Teukolsky, W. T. Vetterling, and B. P. Flannery, *Numerical Recipes: The Art of Scientific Computing*, 3rd ed. (Cambridge University Press, New York, 2007).
[93] H. Bauke and C. H. Keitel, Comput. Phys. Commun. **182**, 2454 (2011).
[94] T. Dziubak and J. Matulewski, Comput. Phys. Commun. **183**, 800 (2012).
[95] X. Antoine, W. Bao, and C. Besse, Comput. Phys. Commun. **184**, 2621 (2013).
[96] N. W. Ashcroft and N. D. Mermin, *Solid State Physics* (Holt, Rinehart and Winston, Austin, TX, 1976).